Article

Cell Reports

Dengue and Zika Virus Cross-Reactive Human Monoclonal Antibodies Protect against Spondweni Virus Infection and Pathogenesis in Mice

Graphical Abstract

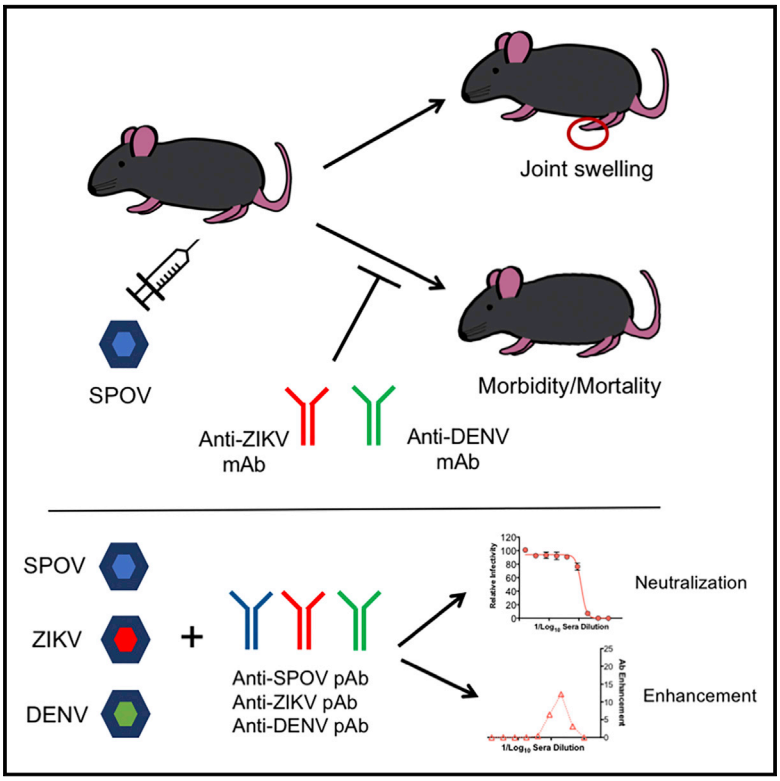

Highlights

- Development of mouse models of SPOV infection
- SPOV uniquely infects feet of mice and results in acute joint swelling
- Serological relatedness between SPOV, ZIKV, and DENV established
- Anti-ZIKV and anti-DENV neutralizing mAbs have protective activity *in vivo*

Authors

Vanessa Salazar, Brett W. Jagger, Juthathip Mongkolsapaya, ..., James E. Crowe, Jr., Gavin R. Screaton, Michael S. Diamond

Correspondence

diamond@wusm.wustl.edu

In Brief

Salazar et al. show that SPOV, the flavivirus most closely related to ZIKV, infects mice when type I interferon signaling is blocked. SPOV causes ankle swelling and infection in the foot, which is more typical of alphaviruses. Human antibodies from ZIKV or DENV subjects protect against lethal SPOV challenge.

Salazar et al., 2019, Cell Reports *26*, 1585–1597
February 5, 2019
https://doi.org/10.1016/j.celrep.2019.01.052

CellPress

Cell Reports
Article

Dengue and Zika Virus Cross-Reactive Human Monoclonal Antibodies Protect against Spondweni Virus Infection and Pathogenesis in Mice

Vanessa Salazar,[1] Brett W. Jagger,[1] Juthathip Mongkolsapaya,[2,3] Katherine E. Burgomaster,[5] Wanwisa Dejnirattisai,[2] Emma S. Winkler,[1,4] Estefania Fernandez,[1,4] Christopher A. Nelson,[4] Daved H. Fremont,[4,9] Theodore C. Pierson,[5] James E. Crowe, Jr.,[6,7,8] Gavin R. Screaton,[2] and Michael S. Diamond[1,4,9,10,11,*]

[1]Department of Medicine, Washington University School of Medicine, Saint Louis, MO 63110, USA
[2]Nuffield Department of Medicine, John Radcliffe Hospital, University of Oxford, Oxford OX3 9DU, UK
[3]Dengue Hemorrhagic Fever Research Unit, Office for Research and Development, Siriraj Hospital, Faculty of Medicine, Mahidol University, Bangkok 10700, Thailand
[4]Department of Pathology & Immunology, Washington University School of Medicine, Saint Louis, MO 63110, USA
[5]Laboratory of Viral Diseases, National Institute of Allergy and Infectious Diseases, NIH, Bethesda, MD 20892, USA
[6]Department of Pediatrics, Vanderbilt University Medical Center, Nashville, TN 37232, USA
[7]Pathology, Microbiology and Immunology, Vanderbilt University Medical Center, Nashville, TN 37232, USA
[8]Vanderbilt Vaccine Center, Vanderbilt University Medical Center, Nashville, TN 37232, USA
[9]Department of Molecular Microbiology, Washington University School of Medicine, Saint Louis, MO 63110, USA
[10]The Andrew M. and Jane M. Bursky Center for Human Immunology and Immunotherapy Programs, Washington University School of Medicine, Saint Louis, MO 63110, USA
[11]Lead Contact
*Correspondence: diamond@wusm.wustl.edu
https://doi.org/10.1016/j.celrep.2019.01.052

SUMMARY

Spondweni virus (SPOV) is the flavivirus that is most closely related to Zika virus (ZIKV). Although SPOV causes sporadic human infections in Africa, recently it was found in *Culex* mosquitoes in Haiti. To investigate the pathogenic spectrum of SPOV, we developed infection models in mice. Although two SPOV strains failed to cause disease in immunocompetent mice, each accumulated in the brain, spleen, eye, testis, and kidney when type I interferon signaling was blocked and unexpectedly caused infection, immune cell infiltration, and swelling in the ankle. In pregnant mice, SPOV replicated in the placenta and fetus but did not cause placental insufficiency or microcephaly. We identified human antibodies from ZIKV or DENV immune subjects that neutralized SPOV infection and protected against lethal challenge. Our experiments describe similarities and differences in clinical syndromes between SPOV and ZIKV and suggest that their serological relatedness has implications for antibody therapeutics and flavivirus vaccine development.

INTRODUCTION

Spondweni virus (SPOV), a member of the same serogroup as Zika virus (ZIKV), is a mosquito-transmitted flavivirus that historically has circulated in sub-Saharan Africa. In 1952, the Chuku strain of SPOV was isolated from a patient in Nigeria, but cross-reactivity in neutralization tests led to its initial misclassification as a ZIKV strain. Until subsequent analysis clarified the identity of SPOV-Chuku (Draper, 1965), the 1955 South African SPOV-SA Ar94 mosquito isolate was considered the prototype SPOV strain (Kokernot et al., 1957; MacNamara, 1954). Although most symptomatic SPOV infections result in mild illness, a subset of cases are believed to progress to more serious disease, including vascular leakage and neurological involvement (Haddow and Woodall, 2016).

The enzootic cycle of SPOV is not entirely defined, but it is likely propagated between mosquitoes and non-human primates (Haddow et al., 2016). In contrast to other flaviviruses (e.g., Dengue, Zika, and West Nile viruses), SPOV infection and dissemination historically was low or non-existent in *Aedes aegypti*, *Aedes albopictus*, and *Culex quinquefasciatus* mosquitoes following infectious blood feeding of SPOV strains (Haddow et al., 2016). However, isolations of SPOV from eight other species of mosquitoes in the genera Aedes, Culex, Eretmapodites, and Mansonia have been reported. Based on its vector biology, it has been speculated that SPOV has limited potential for urban epidemic cycles (Haddow et al., 2016). However, the epidemiology may be changing, as recently, SPOV was detected in field-caught *Culex quinquefasciatus* mosquitoes in Haiti in 2016 (White et al., 2018).

SPOV has a positive-sense, single-stranded RNA genome of approximately 11 kb in length (Pierson and Diamond, 2013). SPOV-Chuku and SPOV-SA Ar94 share ~98% nucleotide and 99% amino acid identity to each other and ~68% nucleotide and 75% amino acid identity to ZIKV, the closest flavivirus relative (Haddow et al., 2016). Sequencing of RNA from SPOV-infected mosquitoes from Haiti revealed 96.8% and 98.8% nucleotide and 98.3% and 98.8% amino acid identity with

SPOV-Chuku and SPOV-SA Ar94 strains, respectively (White et al., 2018). Despite the close genetic relationship to ZIKV, little is known regarding the pathogenesis of SPOV infections and its clinical syndromes.

Here, we investigated the tropism and disease potential of SPOV in mice. SPOV, like ZIKV (Lazear et al., 2016; Rossi et al., 2016), did not replicate efficiently in wild-type (WT) C57BL/6 immunocompetent mice after subcutaneous inoculation. However, administration of an anti-Ifnar1 blocking monoclonal antibody (mAb) rendered animals susceptible to infection and disease by the two prototype strains, SPOV-Chuku and SPOV-SA Ar94. Mice treated with anti-Ifnar1 mAb sustained high levels of SPOV infection in multiple tissues, including serum, spleen, kidney, and brain at 7, 14, and 21 days post-infection (dpi). Unexpectedly, persistent viral RNA was measured in the serum up to 56 dpi, and this finding occurred despite the induction of adaptive B and T cell responses. Moreover, both SPOV strains had the capacity to induce foot swelling, which is not typical of flaviviruses and is instead reminiscent of the musculoskeletal disease observed following alphavirus infection (Morrison et al., 2011). We also assessed the ability of SPOV to infect the placenta and developing fetus in the context of pregnancy. Although SPOV was detected in the placenta and fetal head at embryonic day (E)13.5, overt fetal pathology was not observed. Finally, our studies discerned the serological relatedness of SPOV, ZIKV, and DENV and established that cross-reactive anti-ZIKV and anti-DENV human mAbs can neutralize SPOV infection in cell culture and protect against disease *in vivo*. Collectively, our studies establish disease models of SPOV pathogenesis in mice and define potential protective countermeasures with therapeutic antibodies.

RESULTS

SPOV Pathogenesis in Mice

To begin to understand whether SPOV causes a similar disease pathogenesis to the closely related ZIKV, we developed a mouse model of infection. Although a recent study used AG129 mice lacking both type I interferon (IFN) (α/β) and II IFN (γ) receptors to assess SPOV tropism in the male reproductive tract (McDonald et al., 2017), we sought to establish a less immunocompromised model, which might have greater utility in evaluating viral pathogenesis and host immune responses. Groups of 8-week-old male C57BL/6 mice were treated with an anti-Ifnar1-blocking mAb (MAR1-5A3) 1 day prior to subcutaneous inoculation in the foot with prototype SPOV strains SA Ar94 (South Africa, 1955) or Chuku (Nigeria, 1952; Figure 1). Of note, contemporary infectious isolates from Haiti are not yet available. We confirmed the identity of SPOV SA Ar94 and SPOV-Chuku strains by next-generation sequencing and also established that no other adventitious pathogens were present in our viral stocks. Mice that did not receive anti-Ifnar1 mAb exhibited no weight loss, morbidity, or mortality after inoculation with either SPOV strain (Figures 1A–1D). In comparison, mice inoculated with SPOV-SA Ar94 and pretreated with 0.5, 1, or 2 mg of anti-Ifnar1 mAb had 33%, 66%, and 100% mortality rates, respectively (Figure 1A). Mice inoculated with SPOV-Chuku had lethality rates of 66%–90% when pretreated with 0.5 or 1 mg of anti-Ifnar1 mAb (Figure 1C). Consistent with these results, mice that ultimately succumbed to infection began to lose weight by 5 dpi with either SPOV-SA Ar94 or SPOV-Chuku. By 9 (SPOV-SA Ar94) or 12 (SPOV-Chuku) dpi, animals had lost between 15% and 30% of their starting body weight (Figures 1B and 1D). We also investigated the pathogenic potential of SPOV in 3-week-old male mice in which the human *STAT2* gene was introduced into the mouse *STAT2* locus (hSTAT2 KI) in the absence of anti-Ifnar1 mAb treatment; these mice were tested because they enabled ZIKV to overcome murine innate immune restriction and cause pathogenesis (Gorman et al., 2018). However, unlike ZIKV, SPOV NS5 protein did not promote degradation of human STAT2; nonetheless, SPOV NS5 did bind human STAT2, which could antagonize its innate immune functions through other mechanisms (Grant et al., 2016). In contrast to results with ZIKV, hSTAT2 KI mice did not exhibit weight loss, morbidity, or mortality and sustained little viral infection at 7 dpi with SPOV-SA Ar94 (Figure S1).

In the course of the infection studies of WT C57BL/6 mice, we noticed swelling in the feet of mice inoculated with SPOV-SA Ar94 (Figures 1E and 1F) or SPOV-Chuku (Figures 1G and 1H). SPOV-SA Ar94 caused modest swelling (10%–20% increase in size) in the ipsilateral foot at 5 dpi and only when anti-Ifnar1 mAb was administered. In comparison, mice infected with SPOV-Chuku and pretreated with 0.5 or 1 mg of anti-Ifnar1 mAb had approximately 50% or 80% increases in ipsilateral foot size at 5 dpi, respectively (Figure 1I). Remarkably, the contralateral foot also developed swelling after SPOV-Chuku infection, with an approximately 10%–20% increase in size at 5 dpi when the mice were pretreated with 0.5 or 1 mg of anti-Ifnar1, respectively. Flow cytometric analysis of the ipsilateral foot at 5 dpi revealed a substantial increase in immune cell infiltration in mice pretreated with 1 mg of anti-Ifnar1 and inoculated with SPOV-Chuku in comparison to mock-infected, anti-Ifnar1-treated control animals (Figure 1J). We observed a greater than 300-fold increase in $CD45^+$ leukocytes in the feet of SPOV-Chuku-infected animals, with markedly higher numbers of monocytes, neutrophils, NK cells, $CD8^+$ T cells, $CD4^+$ T cells, and B cells in the joint-associated tissues.

SPOV Tissue Tropism in Mice

We assessed the tissue tropism of SPOV by measuring the viral burden at 7, 14, and 21 dpi. SPOV strains replicated inefficiently in WT mice without anti-Ifnar1 mAb pretreatment, with levels of viral RNA (Table S1) above background observed consistently only in the ipsilateral foot at 7 dpi. In comparison, mice pretreated with 0.5 or 1 mg of anti-Ifnar1 mAb had approximately 10^3 to 10^5 FFU equivalents/g of SPOV-SA Ar94 or SPOV-Chuku in the serum, brain, spleen, testes, kidney, ileum, and eye at 7 dpi (Figures 2A and 2B). Mice inoculated with SPOV-SA Ar94 or SPOV-Chuku both sustained high levels of SPOV RNA (10^5–10^6 FFU equivalents/g) in the ipsilateral and contralateral feet at 7 dpi. At 14 dpi, mice infected with SPOV-SA Ar94 or SPOV-Chuku and treated with 0.5 mg anti-Ifnar1 mAb generally showed waning titers with a ~10-fold reduction in viral RNA in most tissues compared to 7 dpi (Figures 2C and 2D). By 21 dpi, most mice inoculated with SPOV-SA Ar94 had cleared infection in the ileum and eye yet still showed residual viral RNA in the serum,

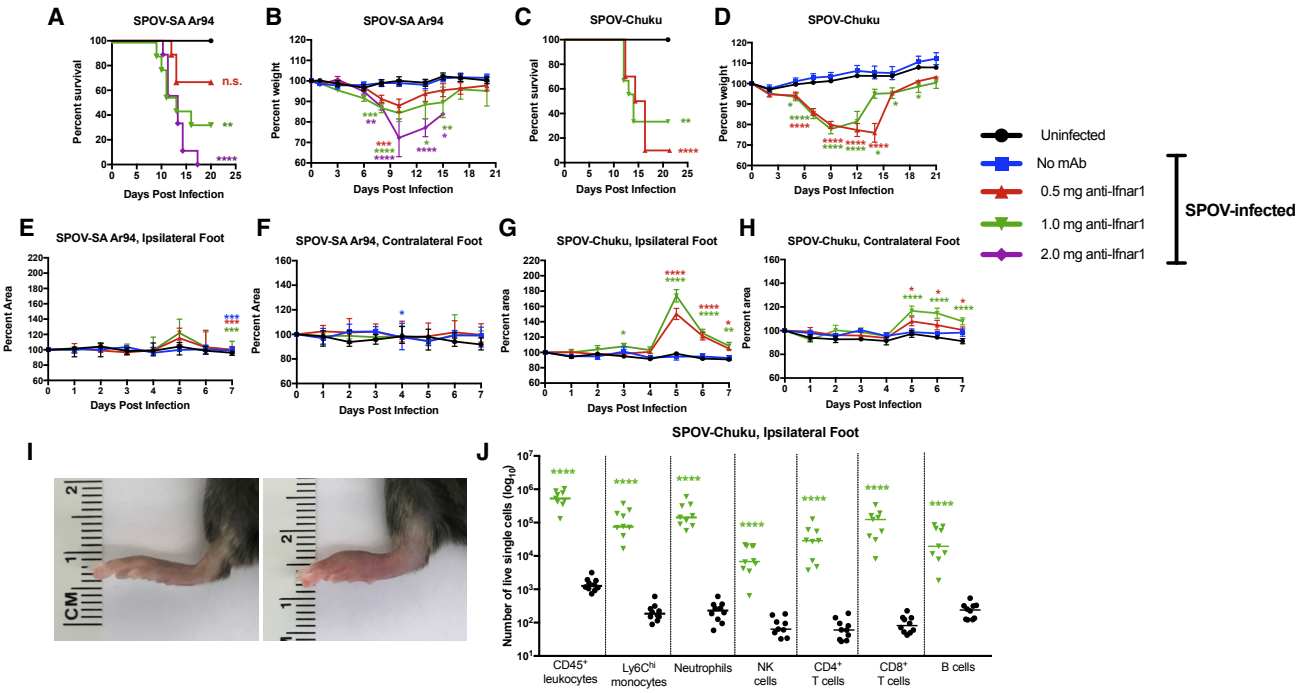

Figure 1. Clinical Consequences of SPOV Infection in Mice

(A–D) Survival and weight loss analysis. 8-week-old C57BL/6 male mice were pretreated at day −1 with no antibody or a single dose of anti-Ifnar1 mAb (0.5, 1, or 2 mg) and then mock-infected or inoculated with 10^6 FFU of SPOV-SA Ar94 (A and B) or 10^5 FFU of SPOV-Chuku (C and D) and followed for survival (A and C) or weight change (B and D). Survival analysis was compared to the uninfected mice (log rank test with Bonferroni post-test: n.s., not significant; $^{**}p < 0.01$; $^{****}p < 0.0001$). Weight change was compared to the uninfected mice (Kruskal-Wallis ANOVA with Dunnett's post-test: $^{*}p < 0.05$; $^{**}p < 0.01$; $^{***}p < 0.001$; $^{****}p < 0.0001$). Data are from two experiments with n = 9 to 10 animals per group. See also Figure S1.

(E–H) C57BL/6 male mice were inoculated with SPOV-SA Ar94 (E and F) or SPOV-Chuku (G and H) as described above. On days 1–7 post-infection, ipsilateral (E and G) and contralateral (F and H) foot swelling was measured using digital calipers and compared to the day 0 time point (Kruskal-Wallis ANOVA with Dunnett's post-test: $^{*}p < 0.05$; $^{**}p < 0.01$; $^{***}p < 0.001$; $^{****}p < 0.0001$). Data are from two experiments with n = 9 to 10 animals per group.

(I) C57BL/6 male mice were inoculated with SPOV-Chuku, and peak swelling was observed in the ipsilateral foot on day 5. Representative images from uninfected (left) and SPOV-Chuku infected mice (right) are shown.

(J) Flow cytometric analysis of uninfected and SPOV-Chuku-inoculated ipsilateral feet at 5 dpi. Both cohorts of mice received 1 mg of anti-Ifnar1 at day −1. Cell numbers of each immune cell subset were compared (Mann-Whitney test: $^{****}p < 0.0001$). Data are from two experiments with n = 9 to 10 animals per group. For (B), (D), and (E)–(H), error bars indicate SEM. For (J), bars denote median values.

spleen, and brain (Figure 2E). Mice infected with SPOV-Chuku sustained greater viral persistence at 21 dpi in several sites, including the serum, brain, spleen, and feet (Figure 2F). Because of the persistent viremia at 21 dpi, we performed a longitudinal study in mice treated with 0.5 mg of anti-Ifnar1 mAb and inoculated with SPOV-SA Ar94. Remarkably, viremia was detected in serum until approximately 56 dpi (Figure 2G).

T and B Cell Responses to SPOV Infection

Given the unexpected persistence of SPOV in some tissues, we evaluated B and T cell responses and compared them to those observed after ZIKV infection. WT mice were pretreated with 0.5 mg of anti-Ifnar1-blocking mAb, inoculated with SPOV-SA Ar94 or ZIKV (Dakar 41525), and *ex vivo* responses of splenic T cells were assessed 8 days later, utilizing a D^b-restricted immunodominant ZIKV-derived 9-mer peptide ($E_{294–302}$; Elong Ngono et al., 2017) that cross-reacts with SPOV (Figure 3A). The corresponding SPOV E protein peptide has three differences at amino acids 296 (p3 of the peptide: valine to isoleucine), 297 (p4: serine to glycine), and 302 (p9: valine to isoleucine); these changes do not alter or are compatible with anchor residues at p2 and p9 (Falk et al., 1991). Relative to uninfected mice, the numbers of $CD8^+$ T cells expressing the cytotoxicity marker granzyme B were increased and similar between SPOV- and ZIKV-infected mice. The numbers of $CD8^+$ T cells expressing IFNγ after peptide restimulation were increased in ZIKV-infected mice relative to SPOV-infected mice, which could reflect the sequence mismatch of the peptide used for restimulation. Notwithstanding this difference, SPOV-infected mice clearly had a higher number of IFNγ^+ $CD8^+$ T cells than naive mice. Together, with the granzyme B responses, this finding confirmed induction of antigen-specific $CD8^+$ T cell responses in SPOV-infected mice. Differences in the frequency or total number of $CD4^+$ T cells were not observed among the three groups (Figure 3A).

Because of the persistent viremia, we evaluated the humoral immune responses. Initially, we assessed the antiviral antibody response at days 7, 14, and 21 after SPOV-SA Ar94 inoculation of mice that were not treated or treated with anti-Infar1 mAb.

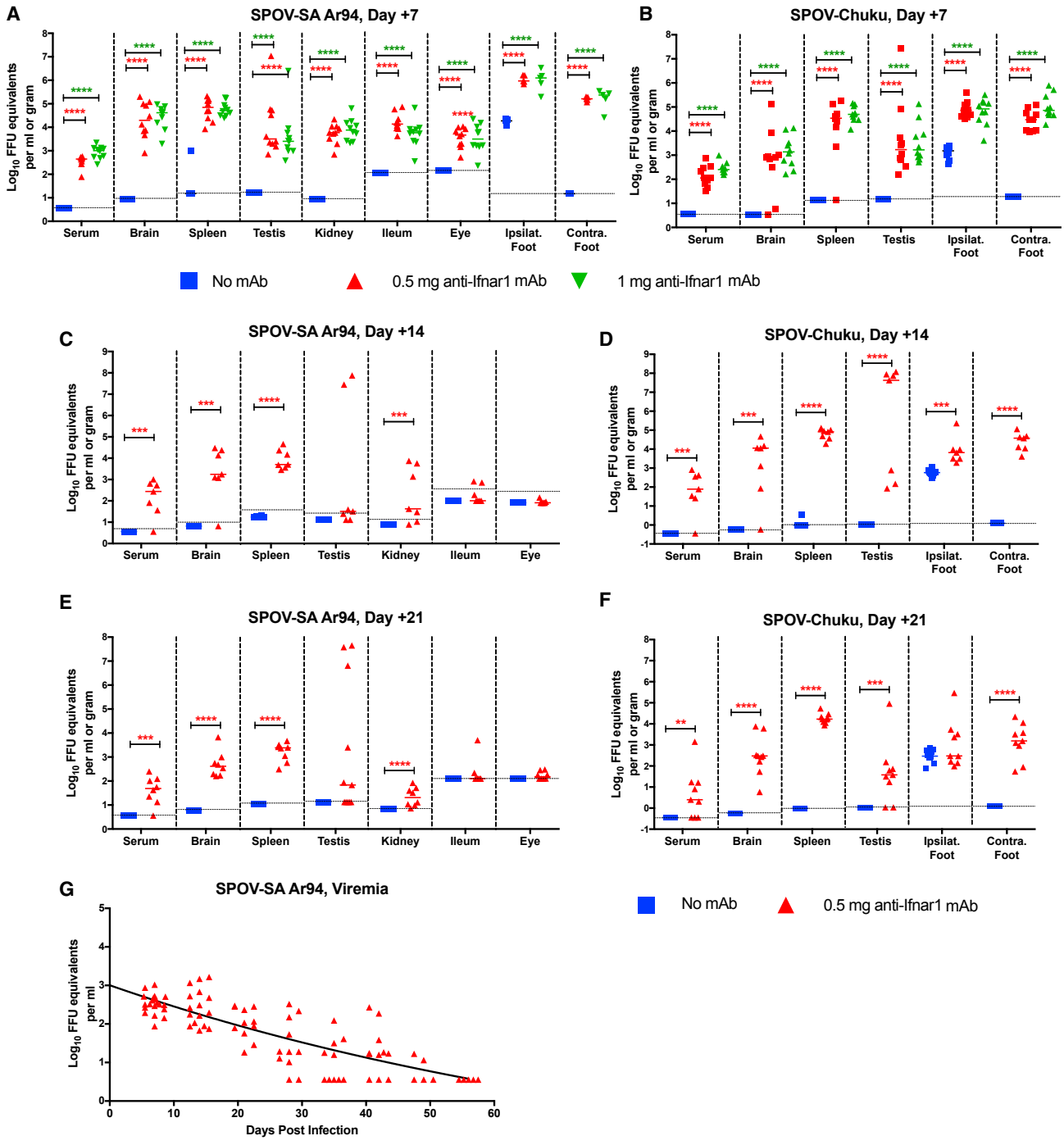

Figure 2. Viral Burden in SPOV-Infected Mice

(A–F) 8-week-old C57BL/6 male mice were pretreated at day −1 with no antibody or a single dose of anti-Ifnar1 mAb (0.5 or 1 mg) and then inoculated with 10^6 FFU of SPOV-SA Ar94 (A, C, and E) or 10^5 FFU of SPOV-Chuku (B, D, and F). Serum and tissues (brain, spleen, testis, kidney, ileum, and eye) were harvested at days 7 (A and B), 14 (C and D), or 21 (E and F) after infection, and SPOV RNA levels were measured by qRT-PCR. Viral RNA levels were compared to tissues from the no anti-Ifnar1 mAb-treated mice (one-way ANOVA with Dunnett's post-test: ***$p < 0.001$; ****$p < 0.0001$). Data are from two experiments: day 7, n = 10; day 14, n = 7 to 10; and day 21, n = 8–10. Bars denote median values.

(G) Mice were pre-treated at day −1 with a single dose of anti-Ifnar1 mAb (0.5 mg) and then inoculated with 10^6 FFU of SPOV-SA Ar94. Serum was collected on the indicated days, and SPOV RNA was measured by qRT-PCR. Data are from two experiments with n = 5–20 animals per time point. Data points on the dotted lines were not measurable and given the arbitrary value of the limit of detection (LOD).

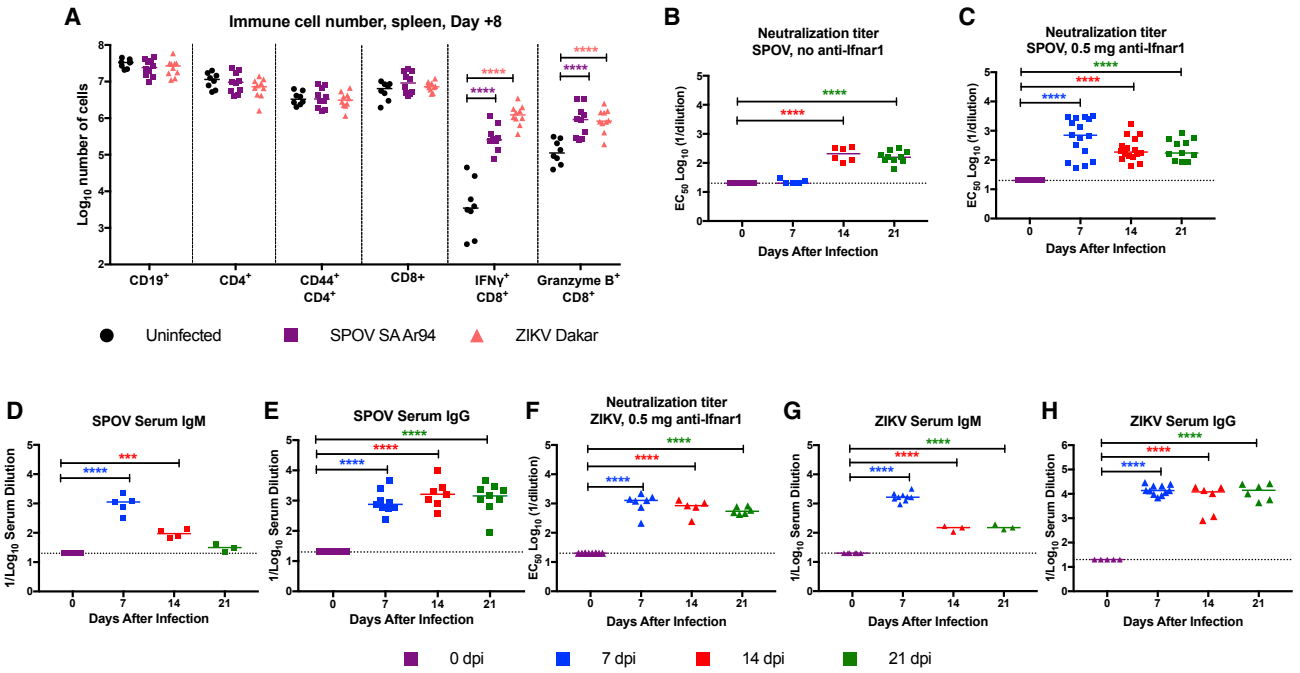

Figure 3. Immune Responses after SPOV or ZIKV Infection

8-week-old C57BL/6 male mice were uninfected or pretreated at day −1 with a single 0.5-mg dose of anti-Ifnar1 mAb and then inoculated with 10^6 FFU of SPOV-SA Ar94 or ZIKV Dakar 41525.

(A) At 8 dpi, spleens were harvested and processed by flow cytometry. The total number of indicated cell populations ($CD19^+$, $CD4^+$, $CD44^+$ $CD4^+$, $CD8^+$, and granzyme B^+ $CD8^+$) is shown. Cells also were incubated with an immunodominant $CD8^+$ T cell peptide and stained intracellularly for IFN-γ. Cell numbers were compared to those obtained from uninfected mice (one-way ANOVA with Dunnett's post-test: $^{**}p < 0.01$; $^{***}p < 0.001$; $^{****}p < 0.0001$). Data are from three experiments with n = 8–10 mice per group.

(B–E) Antibody responses after SPOV infection. Mice were pretreated at day −1 with no mAb (B) or a single 0.5-mg dose of anti-Ifnar1 mAb (C–E) and then inoculated with 10^6 FFU of SPOV-SA Ar94. Serum was harvested at days 0, 7, 14, and 21 after infection and processed for neutralizing activity (B and C) or anti-SPOV IgM (D) and anti-SPOV IgG (E) binding to recombinant SPOV E protein. Data are from two experiments with n = 3–9 mice per group.

(F–H) Antibody responses after ZIKV infection. Mice were pretreated at day −1 with a single 0.5-mg dose of anti-Ifnar1 mAb and then inoculated with 10^6 FFU of ZIKV-Dakar 41525. Serum was harvested at days 0, 7, 14, and 21 after infection and processed for neutralizing activity (F) or anti-ZIKV IgM (G) and anti-ZIKV IgG (H) binding to recombinant ZIKV E protein. Data are from two experiments with n = 3–11 mice per group.

Neutralization and binding data in (B)–(H) were compared to day 0 samples (one-way ANOVA with Dunnett's post-test: $^{**}p < 0.01$; $^{***}p < 0.001$; $^{****}p < 0.0001$). Data points on the dotted lines were not measurable and given the arbitrary value of the LOD. In this figure, bars denote median values.

Serum from mice that did not receive anti-Ifnar1 mAb had higher neutralizing antibody titers at 14 and 21 dpi compared to 0 and 7 dpi (Figure 3B). Serum from mice treated with 0.5 mg of anti-Ifnar1 mAb prior to SPOV-SA Ar94 infection showed neutralizing activity at 7 dpi, which plateaued thereafter (Figure 3C). To extend these findings, in animals infected with SPOV and treated with anti-Ifnar1 mAb, we measured the antiviral immunoglobulin M (IgM) and IgG responses in serum by ELISA using purified, recombinant ectodomain (amino acids 2–412) of SPOV E protein (Figures 3D and 3E). IgM levels peaked at 7 dpi and then decreased over time, whereas IgG levels peaked at 14 dpi and were similar at 21 dpi. As the lack of augmentation of the anti-SPOV IgG response after day 14 might contribute to the persistent viremia, we compared the antibody response after ZIKV infection, where viremia in serum is cleared within 21 dpi (Govero et al., 2016). However, similar to SPOV, serum from ZIKV-infected mice pretreated with anti-Ifnar1-blocking mAb reached peak neutralizing antibody titer at 7 dpi and did not increase further at 14 and 21 dpi (Figure 3F). An ELISA with purified ZIKV E ectodomain protein showed peak IgM levels at 7 dpi (Figure 3G) and constant levels of ZIKV-specific IgG levels at 7, 14, and 21 dpi (Figure 3H), results that were analogous to those seen after SPOV infection. Thus, in mice treated with anti-Ifnar1 mAb, SPOV and ZIKV infection induced similar humoral responses, yet viremia persisted for a longer duration after SPOV infection.

SPOV Infection during Pregnancy

To determine whether SPOV has a similar potential for causing placental damage and fetal demise as ZIKV, we adapted a model of ZIKV infection during pregnancy (Miner et al., 2016). WT dams were treated with either 0, 0.5, or 1 mg of anti-Ifnar1 mAb on E5.5, inoculated with SPOV-SA Ar94 on E6.5 via footpad injection, and maternal and fetal tissues were collected on E13.5 (Figure 4). The levels of SPOV RNA roughly correlated with the dose of anti-Ifnar1 mAb administered, with a trend toward higher levels of SPOV RNA in the serum and brain in dams receiving the 1 mg dose. However, levels of SPOV RNA in the spleen at

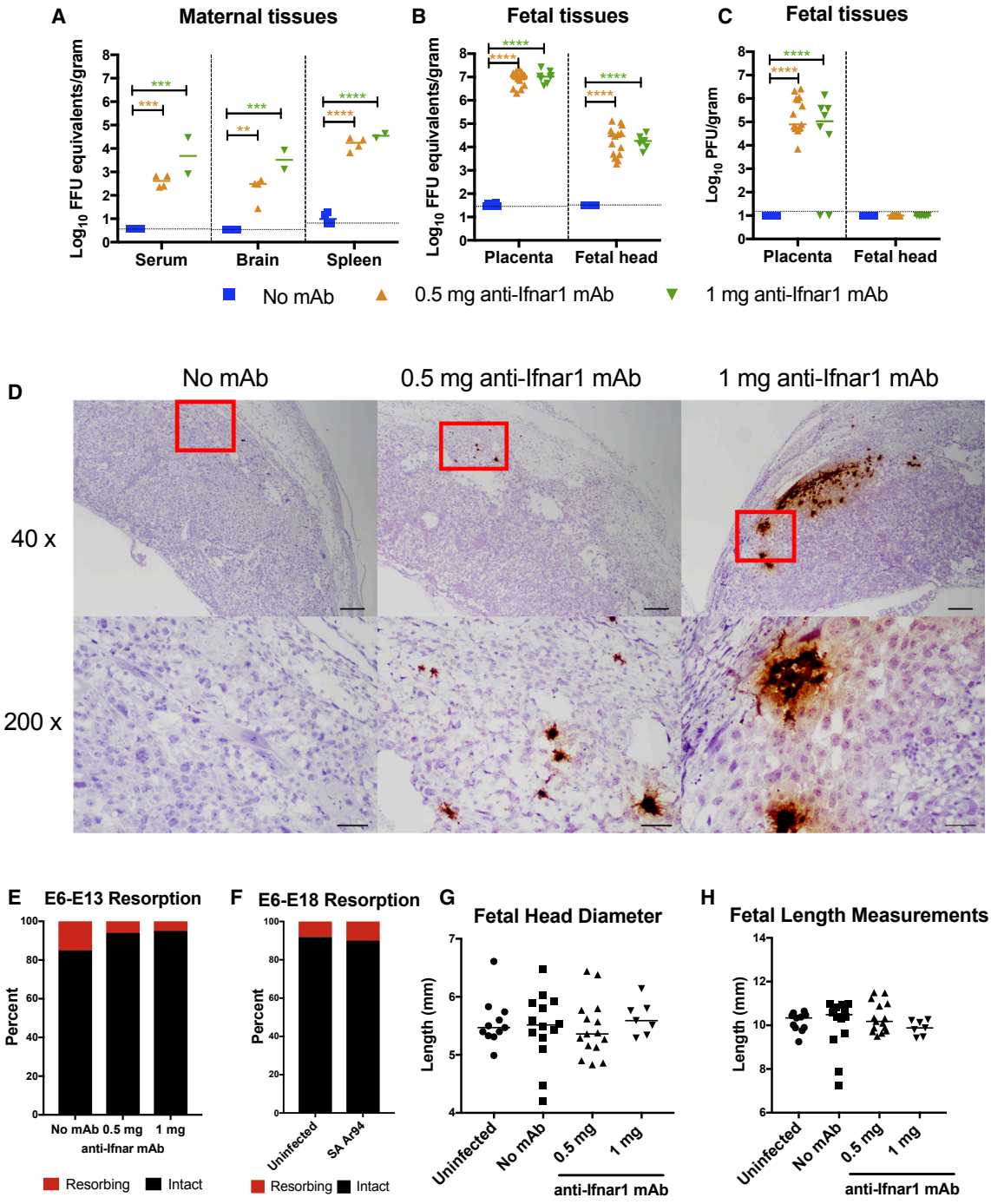

Figure 4. SPOV Infection at the Maternal-Fetal Interface

(A–C) 8- to 10-week-old pregnant C57BL/6 dams were treated on E5.5 with no mAb or anti-Ifnar1 mAb (0.5 or 1 mg) and then inoculated via subcutaneous route with 10^6 FFU of SPOV-SA Ar94 on E6.5. At E13.5, maternal (A) and fetal (B and C) tissues were processed for SPOV RNA (A and B) or infectious virus (C) by qRT-PCR and plaque assays, respectively. Levels of viral RNA or infectious virus were compared to those obtained from mice treated with no mAb (one-way ANOVA with Dunnett's post-test: $^{**}p < 0.01$; $^{***}p < 0.001$; $^{****}p < 0.0001$). Data are from two experiments: n = 4, 4, and 2 dams for the 0-, 0.5-, and 1-mg anti-Ifnar1 groups; n = 14, 15, and 8 fetuses for the 0-, 0.5-, and 1-mg anti-Ifnar1 mAb groups.

(D) RNA ISH staining of placentas at E13.5 from SPOV-infected dams. Low-power (40×: scale bars represent 200 μm) and high-power (200×: scale bars represent 50 μm) images are presented in sequence (top and bottom panels). The images are representative of placentas from 2 to 3 dams.

(legend continued on next page)

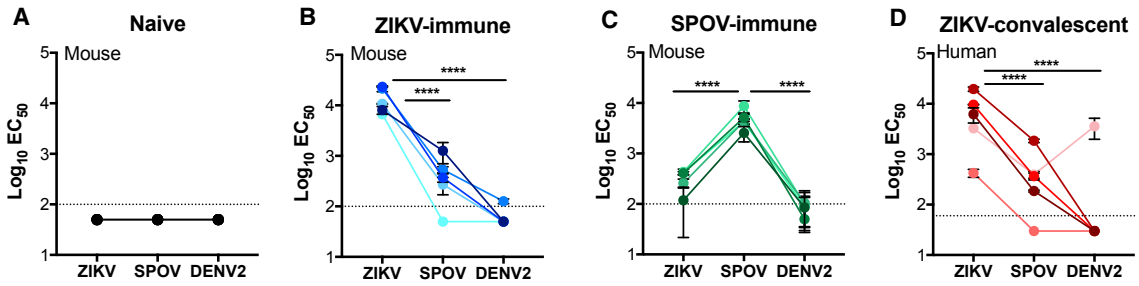

Figure 5. Serological Relatedness of SPOV, ZIKV, and DENV

Neutralization assays were performed using ZIKV, SPOV, and DENV2 GFP reporter virus particles (RVPs). Serial dilutions of sera from naive (A), immune mice after ZIKV (B) or SPOV infection (C), or ZIKV convalescent humans (D) were incubated with indicated RVPs and used to infect a DC-SIGNR-expressing Raji cell line. GFP-expressing cells were measured by flow cytometry at 24–48 h post-infection, depending on the virus. Nonlinear regression analysis was used to determine the dilution of sera at half-maximal neutralization of infection (EC_{50}). Line graphs represent reciprocal EC_{50} titers for individual serum samples against indicated viral strains (mouse serum: naive [n = 4], ZIKV-infected [n = 5], and SPOV-infected [n = 5]; human serum: ZIKV convalescent [n = 5]). Mean EC_{50} was analyzed by two-way ANOVA with Tukey's post-test (****$p < 0.0001$). Error bars indicate the SEM from two experiments of duplicate technical replicates. Dotted lines represent the limit of detection (1:100 dilution for mouse sera; 1:60 dilution for human sera). See also Figures S2, S3, and S4.

7 dpi were similar in dams receiving 0.5 or 1 mg of anti-Ifnar1 mAb (Figure 4A). Dams that did not receive anti-Ifnar1 mAb sustained minimal or no SPOV infection in maternal or fetal tissues. Dams treated with anti-Ifnar1 mAb and inoculated with SPOV showed placental infection and vertical transmission to the developing fetus. Generally, higher amounts of SPOV RNA were detected in the placentas compared to the fetal heads (Figure 4B), and infectious virus ($\sim 10^5$–10^6 plaque-forming units [PFU]/g) was recovered only from the placentas and not the fetal heads (Figure 4C).

Given the high levels of SPOV RNA in the placenta yet relatively low levels in fetal heads, we performed RNA *in situ* hybridization (ISH) to better define the tropism of infection. We detected isolated SPOV RNA-positive cells that localized predominantly to the junctional zone of the placenta in dams treated with anti-Ifnar1 mAb (Figure 4D). This pattern of viral RNA staining is similar to ZIKV infection at a similar gestational time point (Jagger et al., 2017). However, we did not observe significant differences in the fraction of resorbed fetuses in the SPOV-infected dams at E13.5 or E18 relative to the uninfected dams (Figures 4E and 4F). There also were no differences in occipital-frontal fetal head diameter or fetus length at E13.5 when comparing SPOV-infected and uninfected groups (Figures 4G and 4H). Thus, although SPOV is capable of propagating at the maternal-fetal interface, unlike ZIKV (Miner et al., 2016), it does not appear to cause extensive placental damage or fetal demise in mice.

Serological Relatedness of SPOV, ZIKV, and DENV

To confirm the functional relationship of antibody responses to SPOV and explore the potential for cross-neutralization or enhancement of related flaviviruses (e.g., ZIKV and DENV), we tested sera from convalescent mice after ZIKV or SPOV infection for their ability to inhibit SPOV, ZIKV, or DENV2 infection (Figures 5A–5C and S2). Neutralization was evaluated using reporter virus particles (RVPs) produced with the structural proteins of each flavivirus. As expected, naive sera failed to neutralize or enhance SPOV, ZIKV, or DENV2 RVPs (Figures 5A and S2). ZIKV-immune mouse sera strongly neutralized ZIKV (serum dilution EC_{50} of 1/14,049) and moderately neutralized SPOV (EC_{50} of 1/499) but showed little inhibition against DENV2 (EC_{50} < 1/100; Figures 5B and S2). In contrast, SPOV-immune murine sera strongly neutralized SPOV (EC_{50} of 1/5,009) and moderately neutralized ZIKV (EC_{50} of 1/327) but showed little inhibitory activity against DENV2 (EC_{50} < 1/100; Figures 5C and S2). Sub-neutralizing levels of ZIKV- or SPOV-immune sera enhanced infection of all three flaviviruses in cells expressing Fcγ receptors (Figure S2). Because ADE and neutralization of flaviviruses are a function of multiple-hit model of antibody occupancy of the virion, within a given FcγR-expressing cell population near the threshold of neutralization, ADE is observed in some cells whereas neutralization occurs in others (Pierson et al., 2007). These functional data confirm that ZIKV and SPOV are distinct viruses within the same serogroup and that cross-reactive polyclonal antibodies (pAbs) derived from murine infections can enhance ZIKV, SPOV, and DENV infection in cell culture.

We next tested sera from convalescent humans after ZIKV or DENV infection for their ability to inhibit or enhance SPOV, ZIKV, or DENV2 infection (Figures 5D, S3, and S4). Sera from convalescent ZIKV-infected individuals most potently inhibited ZIKV (EC_{50} of 1/7,822), moderately inhibited SPOV (EC_{50} of 1/564),

(E and F) Fetal outcome is presented as frequency of intact versus resorbed fetuses at the time of harvest at E13.5 (E) or E18 (F). The number of fetuses analyzed are as follows: (E) 33, 34, and 20 fetuses for no mAb, 0.5 mg of anti-Ifnar1 mAb, and 1 mg of anti-Ifnar1 mAb, respectively and (F) 37 and 41 fetuses for uninfected and SPOV-infected (after 0.5 mg anti-Ifnar1 treatment), respectively.

(G and H) Measurements of fetal head diameter (G) and length (H). Bars indicate median values. Significance was analyzed by one-way ANOVA with a Dunnett's post-test (all comparisons were not statistically different). Each point represents data from an individual fetus. Data points on the dotted lines were not measurable and given the arbitrary value of the LOD.

For (A)–(C), (G), and (H), bars denote median values.

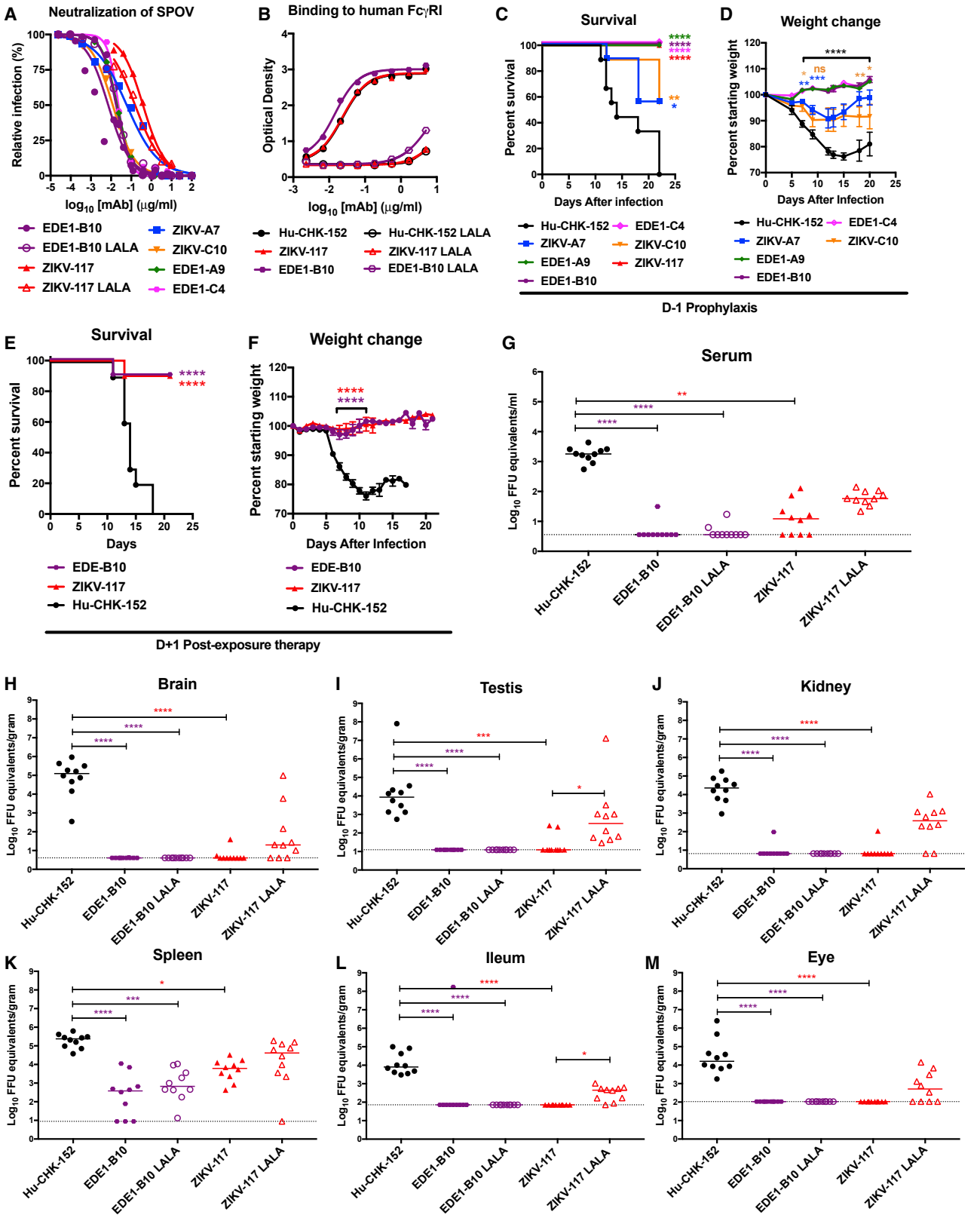

(legend on next page)

and exhibited low neutralizing activity against DENV2 (EC_{50} < 1/60). One individual may have had previous flavivirus exposure, as the serum neutralized ZIKV and DENV2 RVPs at similar titers (EC_{50} of 1/3,568). Sera from convalescent DENV-infected individuals moderately neutralized DENV2 (EC_{50} of 1/337) and weakly inhibited ZIKV (EC_{50} of 1/90) but had little blocking activity against SPOV (EC_{50} < 1/30). In comparison, convalescent human sera from ZIKV- or DENV-infected individuals enhanced infection of all three flaviviruses (Figures S3 and S4).

Anti-DENV and Anti-ZIKV Human mAbs Inhibit SPOV Infection in Mice

Given the serological data, we predicted that a subset of cross-reactive mAbs might neutralize SPOV infection in cell culture and protect *in vivo*. E-dimer epitope (EDE) mAbs isolated from DENV-infected patients bind to an inter-dimer quaternary epitope and cross-neutralize ZIKV infection (Barba-Spaeth et al., 2016; Dejnirattisai et al., 2015, 2016; Fernandez et al., 2017). Indeed, EDE1 mAbs (e.g., EDE1-B10, EDE1-A9, and EDE1-C4) strongly inhibited infection of SPOV in cell culture (EC_{50} of 7, 131, and 23 ng/mL, respectively; Figure 6A). We separately screened a panel of human anti-ZIKV-neutralizing mAbs (Sapparapu et al., 2016) for their ability to inhibit SPOV infection. ZIKV-117 (DII-dimer epitope), ZIKV-A7 (DIII epitope), and ZIKV-C10 (DIII epitope) neutralized SPOV infection (EC_{50} of ~384, 72, and 174 ng/mL, respectively), albeit less efficiently than ZIKV (EC_{50} of ~9, 48, and 403 ng/mL, respectively, against ZIKV-Brazil; Sapparapu et al., 2016). LALA variants of EDE1-B10 and ZIKV-117, which inefficiently engage activating Fcγ receptors (Hessell et al., 2007; Figure 6B), had similar neutralization profiles as their WT counterparts (Figure 6A).

We tested the cross-neutralizing anti-DENV and anti-ZIKV mAbs for their ability to protect mice against SPOV infection. In 8-week-old WT C57BL/6 mice, we passively transferred 1 mg of anti-Ifnar1-blocking mAb and a single 100 μg dose (~4 mg/kg) of EDE1-B10, ZIKV-117, ZIKV-A7, EDE1-A9, EDE1-C4, ZIKV-C10, or an isotype control mAb (hu-CHK-152) 1 day prior to SPOV-SA Ar94 inoculation. Mice treated with EDE1-A9, EDE1-B10, EDE1-C4, and ZIKV-117 were completely protected against lethal infection and weight loss (Figures 6C and 6D). In comparison, mice treated with ZIKV-A7 or ZIKV-C10 were protected only partially with some weight loss and lethality observed.

We evaluated two of the protective mAbs, EDE1-B10 and ZIKV-117, for their efficacy as post-exposure therapy by assessing impact on weight loss, mortality, and SPOV burden in tissues. 8-week-old WT mice were given anti-Ifnar1 mAb 1 day prior to inoculation with SPOV-SA Ar94. Mice treated with a single 100 μg (~4 mg/kg) dose of EDE1-B10 or ZIKV-117 mAbs 1 day after SPOV inoculation sustained no weight loss and low (10%) rates of mortality compared to animals treated with the isotype control hu-CHK-152 mAb (Figures 6E and 6F). We also assessed therapeutic effects on viral burden at 7 dpi using parental or LALA variants of EDE1-B10 or ZIKV-117 mAbs or hu-CHK-152 control mAb (Figures 6G–6M). EDE1-B10 parental and LALA mAbs both controlled infection equivalently with markedly reduced or undetectable viral RNA levels measured in the serum, brain, spleen, testis, kidney, ileum, and eye. This finding suggests that the majority of the protection afforded by EDE1-B10 mAbs is independent of Fc effector functions and likely due to neutralizing activity. ZIKV-117 mAb therapy also reduced SPOV infection in all tissues compared to the control hu-CHK-152 mAb, but the viral RNA levels were higher in the serum and spleen than in EDE1-B10 mAb-treated mice, indicating it was less potent. Unexpectedly, less protection was seen with the ZIKV-117 LALA mAb than parental mAb in the testis (30-fold) and ileum (5-fold), suggesting that, for ZIKV-117, effector functions also contributed to protection.

DISCUSSION

Because SPOV is the most closely related flavivirus to ZIKV, we explored its tropism and pathogenesis in a murine model of infection. Although few human SPOV cases are reported, its incidence may be underestimated through misdiagnosis of infection by more common arthropod-transmitted viruses (Haddow and Woodall, 2016). The study of SPOV is timely, as there is now evidence of introduction into the western hemisphere, with *Culex quinquefasciatus* mosquitoes testing positive for virus in Haiti in 2016 (White et al., 2018). Similar to ZIKV, peripheral infection experiments with two African prototype strains of SPOV resulted

Figure 6. Neutralization and Protection against SPOV Infection by Cross-Reactive Anti-DENV or Anti-ZIKV mAbs

(A) Neutralization of SPOV-SA Ar94 by anti-DENV (EDE1-B10, EDE1-A9, and EDE1-C4) or anti-ZIKV (ZIKV-A7, ZIKV-C10, or ZIKV-117) mAbs as determined by focus reduction neutralization test in Vero cells. LALA variants of EDE1-B10 and ZIKV-117 lacking the ability to bind FcγR also were tested. The data are representative of three experiments, each performed in triplicate.

(B) Binding of parental and LALA variants of hu-CHK-152, ZIKV-117, and EDE1-B10 to human FcγRI (CD64) by ELISA.

(C–F) Prophylaxis and post-exposure treatment studies. 8-week-old C57BL/6 male mice were treated with anti-Ifnar1 mAb at day −1 followed by subcutaneous infection with 10^6 FFU of SPOV-SA Ar94. Mice also were treated at day −1 (prophylaxis) or day +1 (post-exposure) with isotype-control mAb (hu-CHK-152) or with a single 100-μg dose of EDE1-B10, EDE1-A9, EDE1-C4, ZIKV-A7, ZIKV-C10, or ZIKV-117. Survival (C and E) and weight (D and F) data were from two experiments (n = 9 or 10 per group; survival: log rank test with Bonferroni post-test; weight: Kruskal-Wallis ANOVA with Dunnett's post-test). The bracketed bar indicates statistical significance (****$p < 0.0001$) for all mAb groups compared to hu-CHK-152 control mAb at the indicated time points. Colored stars were added for particular mAbs with different statistical significance compared to hu-CHK-152 (*$p < 0.05$; **$p < 0.01$; ***$p < 0.001$).

(G–M) Post-exposure therapeutic studies. 8-week-old WT male mice were treated with anti-Ifnar1 mAb followed by subcutaneous inoculation with SPOV-SA Ar94. At 1 dpi, mice were treated with a single 100-μg dose of isotype-control mAb (CHK-152), EDE1-B10 (parental or LALA), or ZIKV-117 (parental or LALA). At 7 dpi, SPOV RNA was measured in serum (G), brain (H), spleen (I), testis (J), kidney (K), ileum (L), and eye (M). Bars indicate median values collected from two experiments (n = 10 per group). Statistical significance was determined (Kruskal-Wallis ANOVA with Dunn's post-test: *$p < 0.05$; **$p < 0.01$; ***$p < 0.001$; ****$p < 0.0001$).

Data points on the dotted lines were not measurable and given the arbitrary value of the LOD. For (D) and (F), error bars indicate SEM.

in no disease in WT immunocompetent C57BL/6 mice. In contrast, both SPOV strains disseminated widely when mice were given a single dose of anti-Ifnar1-blocking mAb, suggesting that, like ZIKV (Lazear et al., 2016; Rossi et al., 2016), SPOV fails to antagonize the murine type I IFN response. Unlike ZIKV, this cannot be overcome by replacement of mouse Stat2 with human STAT2, as SPOV did not replicate efficiently in hSTAT2-KI mice, whereas ZIKV does (Gorman et al., 2018). In the context of anti-Ifnar1 mAb treatment, both strains of SPOV spread to visceral and CNS tissues, persisted in tissues for weeks, and caused morbidity and mortality in mice. SPOV, like ZIKV (Cugola et al., 2016; Govero et al., 2016; Ma et al., 2016; Miner et al., 2016), was able to infect the testis in males and the placenta in pregnant dams. Thus, at least in immunodeficient mice, SPOV shares tropism features with ZIKV. Because of its genetic and family relatedness, we tested anti-DENV- and anti-ZIKV-neutralizing mAbs for their ability to cross-neutralize SPOV. We identified human mAbs recognizing the EDE epitope on DENV (EDE1-B10) and domain II dimer epitope on ZIKV (ZIKV-117) that neutralized SPOV infection and protected against infection and lethal challenge. Although these data suggest that vaccine or antibody therapy strategies targeting other closely related flaviviruses may inhibit SPOV, our studies are limited by the use of prototypic African strains from the 1950s. As contemporary strains become available, they will need to be evaluated for antibody reactivity and neutralization patterns. The SPOV genome recently detected in Haiti had 98.3% and 98.8% amino acid identity with SPOV-Chuku and SPOV-SA Ar94 strains, respectively (White et al., 2018).

The tissue tropism and pathogenesis of SPOV in mice has not been extensively explored, although historical studies reported virus-induced death in newborn and weanling mice after intracranial inoculation (Kokernot et al., 1957). Our experiments in anti-Ifnar1 mAb-treated adult mice are consistent with a recent report evaluating SPOV-SA Ar94 infection in AG129 mice, which lack the receptors required for both type I and type II IFN signaling (McDonald et al., 2017). In AG129 mice inoculated with SPOV-SA Ar94, nearly uniform mortality was observed after subcutaneous or intraperitoneal inoculation, and this phenotype correlated with high viral burden in the testis, epididymis, and brain at the time of assessment. Our experiments extend these findings in less immunocompromised mice and further define the kinetics of infection and tissue tropism. At 7 days after subcutaneous inoculation with SPOV-SA Ar94 or SPOV-Chuku, we observed high levels of infection in many of the same tissues that ZIKV infects (Lazear et al., 2016), including the spleen, kidney, eye, testis, blood, gastrointestinal tract, and brain. Moreover, at 21 dpi, we detected viral persistence in the brain, spleen, and kidney. In contrast to that seen with ZIKV in mice (Govero et al., 2016; Ma et al., 2016) or in humans (Mansuy et al., 2016a, 2016b), we did not observe persistence of SPOV RNA in the testis. Although ejaculates from SPOV-inoculated AG129 males contained infectious virus, levels were substantially lower than in ZIKV-infected males (McDonald et al., 2017), and thus, the potential for sexual transmission of SPOV may be much less than with ZIKV.

Viremia was prolonged in SPOV-infected mice treated with a single dose of anti-Ifnar1 mAb. Although further studies defining the source of this virus are warranted, persistence in lymphoid tissues and kidneys was noted. Persistent viremia also was observed after ZIKV infection of humans and non-human primates (Aliota et al., 2018; Mansuy et al., 2017; Nguyen et al., 2017), including during pregnancy (Driggers et al., 2016; Goncé et al., 2018; Suy et al., 2016). As persistent ZIKV and SPOV viremia occurs in the setting of induction of neutralizing antibodies and specific $CD8^+$ T cell responses, the immunological basis for failure to control infection remains unexplained.

Analogous to studies with ZIKV (reviewed in Morrison and Diamond, 2017) and more recent experiments with other neurotropic flaviviruses (e.g., West Nile and Powassan viruses; Platt et al., 2018), SPOV efficiently infected anti-Ifnar1 mAb-treated pregnant dams and disseminated to the placenta and fetal head. In contrast to ZIKV (Cugola et al., 2016; Miner et al., 2016; Richner et al., 2017), infection of the placenta and fetus in mice by SPOV was not associated with placental insufficiency, growth retardation, or microcephaly. Given the relatively low levels of SPOV infection in the fetal heads at day 7 after maternal infection, we were unable to define the cellular tropism in the brain by RNA *in situ* hybridization techniques. Indeed, we could not recover infectious SPOV from fetal heads despite detecting viral RNA. Our inability to detect infectious SPOV in the fetal heads may be because (1) virus in the fetus head is neutralized by maternal antibodies that cross the placental barrier and/or (2) the level of infectious virus is below our limit of detection; qRT-PCR of viral RNA is ~100-fold more sensitive. The differential outcomes in fetuses also may be due to differences in tropism of SPOV for certain neuroprogenitor cells or disparity in capacity of SPOV to cause cell injury and death. Notwithstanding the absence of effect on fetal resorption and growth, the long-term neurodevelopmental and behavioral consequences of congenital SPOV infection in the fetal head remain to be assessed.

An unexpected observation was that both SPOV strains caused infection and swelling in the feet of mice, reminiscent of the disease observed following arthritogenic alphavirus infections (Morrison et al., 2011). At 5 dpi, high numbers of leukocytes from multiple immune cell lineages accumulated in joint-associated tissues of SPOV-Chuku-infected mice. Although arthralgia is a commonly described symptom after flavivirus infection in humans (Pierson and Diamond, 2013), frank joint swelling is not typical. Nonetheless, in one study characterizing the ZIKV epidemic in Brazil in 2015, 23% of documented cases had joint swelling (Cerbino-Neto et al., 2016). In a study in India, 4% of DENV-infected individuals experienced acute joint swelling (Taraphdar et al., 2012). Thus, joint swelling appears to occur, albeit with low frequency, with some flavivirus infections. We observed high levels of SPOV-SA Ar94 or SPOV-Chuku infection at 7 dpi in the musculoskeletal tissues of the ipsilateral and contralateral feet. Remarkably, SPOV-Chuku was measurable at 21 dpi, even in mice that had received no blockade of type I IFN signaling. Although further studies are required, we speculate that the early replication in this tissue (immediately after inoculation) could result in local immune evasion that might not occur in other distal tissues where paracrine spread of type I IFN creates an antiviral state. The degree of foot swelling did not correlate directly with viral burden, as greater swelling was observed after

SPOV-Chuku infection, which accumulated to lower levels. As joint swelling after chikungunya virus infection in mice is attributed to the production of pro-inflammatory cytokines and chemokines and infiltration and activation of immune cell subsets (Fox and Diamond, 2016), the differences in phenotype between the two SPOV strains might be explained by distinct inflammatory responses.

Using mouse and human convalescent sera, we confirmed the serological relatedness of SPOV to ZIKV and distance of SPOV to DENV2, as judged by differences in neutralization titers. These results suggest that, in ZIKV-endemic regions (or future ZIKV-vaccinated regions), it may be difficult for SPOV to emerge due to cross-immunity. In contrast, because SPOV and ZIKV immune sera had limited neutralizing activity against DENV, and correspondingly, DENV immune sera had limited inhibitory activity against SPOV infection, SPOV could emerge in DENV-immune or vaccinated regions, contingent on its ability to propagate in mosquito species capable of epidemic transmission.

We also observed reciprocal enhancement of SPOV, ZIKV, and DENV2 infection by the different murine and human sera. Enhanced infection occurs when cross-reactive, non-neutralizing quantities of antibodies bind virus and facilitate infection of cells expressing Fc-γ receptors. A feature of DENV pathogenesis is that antibodies to one serotype can exacerbate infection with a second serotype via antibody-dependent enhancement (Culshaw et al., 2017; Halstead, 1979). Nonetheless, antibody-enhanced infection in cell culture has been demonstrated for many viruses without evidence of worsened disease in humans. Thus, epidemiological evidence from humans will be needed to establish whether clinically relevant enhancement of DENV, ZIKV, or SPOV pathogenesis occurs in the setting of pre-existing heterologous flavivirus immunity.

We evaluated whether particular anti-ZIKV or anti-DENV human neutralizing mAbs could protect against SPOV infection as a prelude for possible future use in humans. Two classes of cross-reactive human Abs (which may not be generated during natural infection by all individuals) showed substantial inhibitory activity against SPOV infection in mice: EDE1 anti-DENV mAbs and ZIKV-117 mAbs. (1) EDE1 mAbs were isolated from DENV-infected patients, are highly neutralizing for multiple DENV serotypes (Dejnirattisai et al., 2015), cross-neutralize ZIKV infection (Barba-Spaeth et al., 2016), and protect against vertical transmission of ZIKV in animal models (Fernandez et al., 2017). EDE1 mAbs engage contact residues in DI, DII, and DIII in the context of a quaternary E protein dimer epitope (Barba-Spaeth et al., 2016; Rouvinski et al., 2015). Our experiments showed potent cross-neutralization of SPOV by the EDE1-B10 mAb and an ability to protect against lethal challenge and control dissemination to distant organs. Moreover, abrogation of interactions with FcγRs and complement components by introduction of a LALA mutation in the Fc domain (Hessell et al., 2007) did not impact therapeutic activity of EDE1-B10, suggesting that the majority of its activity *in vivo* is due to direct neutralization. (2) ZIKV-117 mAb neutralizes ZIKV strains of the African and Asian lineages and can reduce fetal infection and death in mice (Sapparapu et al., 2016). ZIKV-117 binds at the E protein dimer interface, which likely prevents the requisite reorganization of E protein monomers into fusogenic trimers to escape the endosome (Hasan et al., 2017). Initial studies suggested that ZIKV-117 might be virus type specific because it failed to bind to DENV-infected cells or purified WNV E protein (Sapparapu et al., 2016); our study reveals that ZIKV-117 can recognize the more closely related SPOV and inhibit its infection in cell culture. Although ZIKV-117 could protect against SPOV-induced clinical disease, it showed less antiviral activity than EDE1-B10. Moreover, some of the therapeutic activity of ZIKV-117 was lost in the LALA variant, even though *in vitro* neutralization of the parental and LALA versions was virtually identical. Collectively, these results suggest that less potently neutralizing mAbs likely require adjunctive Fc-effector functions to mediate optimal protection *in vivo*.

In summary, we developed a murine model of infection and pathogenesis of SPOV that has similarities and differences with the closely related ZIKV. SPOV does not replicate efficiently in immunocompetent mice after peripheral inoculation, likely due to a failure to antagonize the IFN responses of its non-natural host, the mouse. However, if type I IFN signaling is blocked, SPOV can disseminate to many of the same organs as ZIKV and result in lethal or persistent infection. Uniquely, SPOV infection in the foot resulted in clinically observable swelling and immune cell infiltrates, which are not observed after ZIKV infection in mice. Although SPOV also disseminated to the maternal-fetal interface in pregnant dams, in contrast to ZIKV, it failed to cause extensive placental or fetal injury. Finally, we identified several human cross-reactive mAbs derived from ZIKV- or DENV-infected patients that potently neutralized SPOV infection in cell culture. Our passive transfer studies in mice suggest that some classes of cross-reactive mAbs (e.g., EDE1 mAbs) may have substantial therapeutic activity against SPOV *in vivo*, which may be relevant to vaccine or treatment strategies, should SPOV spread further in the Americas or other continents.

STAR★METHODS

Detailed methods are provided in the online version of this paper and include the following:

- KEY RESOURCES TABLE
- CONTACT FOR REAGENT AND RESOURCE SHARING
- EXPERIMENTAL MODEL AND SUBJECT DETAILS
  - Viruses
  - Recombinant viral proteins
  - Serum from ZIKV- and DENV-immune subjects
  - Ethics statement for mouse studies
  - Mouse infection experiments
- METHOD DETAILS
  - Measurement of viral burden
  - Histology and RNA *in situ* hybridization
  - RVP neutralization and enhancement assays
  - Antibody-virus neutralization assays
  - Antibody responses
  - T cell assays
  - Flow cytometric analysis
- QUANTIFICATION AND STATISTICAL ANALYSIS
  - Data analysis
- DATA AND SOFTWARE AVAILABILITY

SUPPLEMENTAL INFORMATION

Supplemental Information includes four figures and one table and can be found with this article online at https://doi.org/10.1016/j.celrep.2019.01.052.

ACKNOWLEDGMENTS

This work was supported by grants from the NIH (R01 AI073755, R01 AI127828, and R01 HD091218 to M.S.D.; R01 AI127828 to M.S.D. and J.E.C.; T32 AI007163 to E.F.; T32 AI007172 to B.W.J.; and HHSN272201200026C [CSGID] to D.H.F.), the intramural research program of NIAID (T.C.P.), Wellcome Trust to G.R.S., MRC-NEWTON UK to J.M., and The National Institute for Health Research Biomedical Research Centre funding scheme UK. We thank Bin Cao and Indira Mysorekar for tissue processing and Julie Fox for advice on statistical analysis.

AUTHOR CONTRIBUTIONS

V.S., B.W.J., W.D., J.M., J.E.C., T.C.P., G.R.S., and M.S.D. designed the experiments. V.S., E.F., B.W.J., W.D., K.E.B., E.S.W., and J.M. performed the experiments. V.S., B.W.J., W.D., K.E.B., E.S.W., and J.M. performed data analysis. C.A.N., D.H.F., and J.E.C. contributed key reagents. V.S. and M.S.D. wrote the initial draft of the manuscript, with other authors providing comments and edits to the final version.

DECLARATION OF INTERESTS

M.S.D. is a consultant for Inbios and is on the Scientific Advisory Board of Moderna. G.R.S. is on the R&D Advisory Board of GlaxoSmithKline. J.E.C. has served as a consultant for Takeda Vaccines, Sanofi Pasteur, Pfizer, and Novavax; is on the Scientific Advisory Boards of CompuVax, GigaGen, Meissa Vaccines, and PaxVax; and is Founder of IDBiologics.

Received: September 21, 2018
Revised: December 17, 2018
Accepted: January 15, 2019
Published: February 5, 2019

REFERENCES

Aliota, M.T., Dudley, D.M., Newman, C.M., Weger-Lucarelli, J., Stewart, L.M., Koenig, M.R., Breitbach, M.E., Weiler, A.M., Semler, M.R., Barry, G.L., et al. (2018). Molecularly barcoded Zika virus libraries to probe in vivo evolutionary dynamics. PLoS Pathog. *14*, e1006964.

Ansarah-Sobrinho, C., Nelson, S., Jost, C.A., Whitehead, S.S., and Pierson, T.C. (2008). Temperature-dependent production of pseudoinfectious dengue reporter virus particles by complementation. Virology *381*, 67–74.

Barba-Spaeth, G., Dejnirattisai, W., Rouvinski, A., Vaney, M.C., Medits, I., Sharma, A., Simon-Lorière, E., Sakuntabhai, A., Cao-Lormeau, V.M., Haouz, A., et al. (2016). Structural basis of potent Zika-dengue virus antibody cross-neutralization. Nature *536*, 48–53.

Cerbino-Neto, J., Mesquita, E.C., Souza, T.M., Parreira, V., Wittlin, B.B., Durovni, B., Lemos, M.C., Vizzoni, A., Bispo de Filippis, A.M., Sampaio, S.A., et al. (2016). Clinical manifestations of Zika virus infection, Rio de Janeiro, Brazil, 2015. Emerg. Infect. Dis. *22*, 1318–1320.

Cugola, F.R., Fernandes, I.R., Russo, F.B., Freitas, B.C., Dias, J.L., Guimarães, K.P., Benazzato, C., Almeida, N., Pignatari, G.C., Romero, S., et al. (2016). The Brazilian Zika virus strain causes birth defects in experimental models. Nature *534*, 267–271.

Culshaw, A., Mongkolsapaya, J., and Screaton, G.R. (2017). The immunopathology of dengue and Zika virus infections. Curr. Opin. Immunol. *48*, 1–6.

Dejnirattisai, W., Wongwiwat, W., Supasa, S., Zhang, X., Dai, X., Rouvinski, A., Jumnainsong, A., Edwards, C., Quyen, N.T., Duangchinda, T., et al. (2015). A new class of highly potent, broadly neutralizing antibodies isolated from viremic patients infected with dengue virus. Nat. Immunol. *16*, 170–177.

Dejnirattisai, W., Supasa, P., Wongwiwat, W., Rouvinski, A., Barba-Spaeth, G., Duangchinda, T., Sakuntabhai, A., Cao-Lormeau, V.M., Malasit, P., Rey, F.A., et al. (2016). Dengue virus sero-cross-reactivity drives antibody-dependent enhancement of infection with zika virus. Nat. Immunol. *17*, 1102–1108.

Dowd, K.A., DeMaso, C.R., Pelc, R.S., Speer, S.D., Smith, A.R.Y., Goo, L., Platt, D.J., Mascola, J.R., Graham, B.S., Mulligan, M.J., et al. (2016). Broadly neutralizing activity of Zika virus-immune sera identifies a single viral serotype. Cell Rep. *16*, 1485–1491.

Draper, C.C. (1965). Infection with the Chuku strain of Spondweni virus. West Afr. Med. J. *14*, 16–19.

Driggers, R.W., Ho, C.Y., Korhonen, E.M., Kuivanen, S., Jääskeläinen, A.J., Smura, T., Rosenberg, A., Hill, D.A., DeBiasi, R.L., Vezina, G., et al. (2016). Zika virus infection with prolonged maternal viremia and fetal brain abnormalities. N. Engl. J. Med. *374*, 2142–2151.

Elong Ngono, A., Vizcarra, E.A., Tang, W.W., Sheets, N., Joo, Y., Kim, K., Gorman, M.J., Diamond, M.S., and Shresta, S. (2017). Mapping and role of the $CD8^+$ T cell response during primary Zika virus infection in mice. Cell Host Microbe *21*, 35–46.

Falk, K., Rötzschke, O., Stevanović, S., Jung, G., and Rammensee, H.G. (1991). Allele-specific motifs revealed by sequencing of self-peptides eluted from MHC molecules. Nature *351*, 290–296.

Fernandez, E., Dejnirattisai, W., Cao, B., Scheaffer, S.M., Supasa, P., Wongwiwat, W., Esakky, P., Drury, A., Mongkolsapaya, J., Moley, K.H., et al. (2017). Human antibodies to the dengue virus E-dimer epitope have therapeutic activity against Zika virus infection. Nat. Immunol. *18*, 1261–1269.

Fox, J.M., and Diamond, M.S. (2016). Immune-mediated protection and pathogenesis of chikungunya virus. J. Immunol. *197*, 4210–4218.

Goncé, A., Martínez, M.J., Marbán-Castro, E., Saco, A., Soler, A., Alvarez-Mora, M.I., Peiro, A., Gonzalo, V., Hale, G., Bhatnagar, J., et al. (2018). Spontaneous abortion associated with Zika virus infection and persistent viremia. Emerg. Infect. Dis. *24*, 933–935.

Gorman, M.J., Caine, E.A., Zaitsev, K., Begley, M.C., Weger-Lucarelli, J., Uccellini, M.B., Tripathi, S., Morrison, J., Yount, B.L., Dinnon, K.H., 3rd., et al. (2018). An immunocompetent mouse model of Zika virus infection. Cell Host Microbe *23*, 672–685.e6.

Govero, J., Esakky, P., Scheaffer, S.M., Fernandez, E., Drury, A., Platt, D.J., Gorman, M.J., Richner, J.M., Caine, E.A., Salazar, V., et al. (2016). Zika virus infection damages the testes in mice. Nature *540*, 438–442.

Grant, A., Ponia, S.S., Tripathi, S., Balasubramaniam, V., Miorin, L., Sourisseau, M., Schwarz, M.C., Sánchez-Seco, M.P., Evans, M.J., Best, S.M., and García-Sastre, A. (2016). Zika virus targets human STAT2 to inhibit type I interferon signaling. Cell Host Microbe *19*, 882–890.

Haddow, A.D., and Woodall, J.P. (2016). Distinguishing between Zika and Spondweni viruses. Bull. World Health Organ. *94*, 711–711A.

Haddow, A.D., Nasar, F., Guzman, H., Ponlawat, A., Jarman, R.G., Tesh, R.B., and Weaver, S.C. (2016). Genetic characterization of Spondweni and Zika viruses and susceptibility of geographically distinct strains of Aedes aegypti, Aedes albopictus and Culex quinquefasciatus (Diptera: Culicidae) to Spondweni virus. PLoS Negl. Trop. Dis. *10*, e0005083.

Halstead, S.B. (1979). In vivo enhancement of dengue virus infection in rhesus monkeys by passively transferred antibody. J. Infect. Dis. *140*, 527–533.

Hasan, S.S., Miller, A., Sapparapu, G., Fernandez, E., Klose, T., Long, F., Fokine, A., Porta, J.C., Jiang, W., Diamond, M.S., et al. (2017). A human antibody against Zika virus crosslinks the E protein to prevent infection. Nat. Commun. *8*, 14722.

Hessell, A.J., Hangartner, L., Hunter, M., Havenith, C.E., Beurskens, F.J., Bakker, J.M., Lanigan, C.M., Landucci, G., Forthal, D.N., Parren, P.W., et al. (2007). Fc receptor but not complement binding is important in antibody protection against HIV. Nature *449*, 101–104.

Jagger, B.W., Miner, J.J., Cao, B., Arora, N., Smith, A.M., Kovacs, A., Mysorekar, I.U., Coyne, C.B., and Diamond, M.S. (2017). Gestational Stage and IFN-lambda Signaling Regulate ZIKV Infection In Utero. Cell Host Microbe *22*, 366–376.e363.

Kokernot, R.H., Smithburn, K.C., Muspratt, J., and Hodgson, B. (1957). Studies on arthropod-borne viruses of Tongaland. VIII. Spondweni virus, an agent previously unknown, isolated from Taeniorhynchus (Mansonioides) uniformis. S. Afr. J. Med. Sci. *22*, 103–112.

Lanciotti, R.S., Kosoy, O.L., Laven, J.J., Velez, J.O., Lambert, A.J., Johnson, A.J., Stanfield, S.M., and Duffy, M.R. (2008). Genetic and serologic properties of Zika virus associated with an epidemic, Yap State, Micronesia, 2007. Emerg. Infect. Dis. *14*, 1232–1239.

Lazear, H.M., Govero, J., Smith, A.M., Platt, D.J., Fernandez, E., Miner, J.J., and Diamond, M.S. (2016). A mouse model of Zika virus pathogenesis. Cell Host Microbe *19*, 720–730.

Ma, W., Li, S., Ma, S., Jia, L., Zhang, F., Zhang, Y., Zhang, J., Wong, G., Zhang, S., Lu, X., et al. (2016). Zika virus causes testis damage and leads to male infertility in mice. Cell *167*, 1511–1524.e10.

MacNamara, F.N. (1954). Zika virus: a report on three cases of human infection during an epidemic of jaundice in Nigeria. Trans. R. Soc. Trop. Med. Hyg. *48*, 139–145.

Mansuy, J.M., Pasquier, C., Daudin, M., Chapuy-Regaud, S., Moinard, N., Chevreau, C., Izopet, J., Mengelle, C., and Bujan, L. (2016a). Zika virus in semen of a patient returning from a non-epidemic area. Lancet Infect. Dis. *16*, 894–895.

Mansuy, J.M., Suberbielle, E., Chapuy-Regaud, S., Mengelle, C., Bujan, L., Marchou, B., Delobel, P., Gonzalez-Dunia, D., Malnou, C.E., Izopet, J., and Martin-Blondel, G. (2016b). Zika virus in semen and spermatozoa. Lancet Infect. Dis. *16*, 1106–1107.

Mansuy, J.M., Mengelle, C., Pasquier, C., Chapuy-Regaud, S., Delobel, P., Martin-Blondel, G., and Izopet, J. (2017). Zika virus infection and prolonged viremia in whole-blood specimens. Emerg. Infect. Dis. *23*, 863–865.

McDonald, E.M., Duggal, N.K., and Brault, A.C. (2017). Pathogenesis and sexual transmission of Spondweni and Zika viruses. PLoS Negl. Trop. Dis. *11*, e0005990.

Miner, J.J., Cao, B., Govero, J., Smith, A.M., Fernandez, E., Cabrera, O.H., Garber, C., Noll, M., Klein, R.S., Noguchi, K.K., et al. (2016). Zika virus infection during pregnancy in mice causes placental damage and fetal demise. Cell *165*, 1081–1091.

Morrison, T.E., and Diamond, M.S. (2017). Animal models of Zika virus infection, pathogenesis, and immunity. J. Virol. *91*, e00009-17.

Morrison, T.E., Oko, L., Montgomery, S.A., Whitmore, A.C., Lotstein, A.R., Gunn, B.M., Elmore, S.A., and Heise, M.T. (2011). A mouse model of chikungunya virus-induced musculoskeletal inflammatory disease: evidence of arthritis, tenosynovitis, myositis, and persistence. Am. J. Pathol. *178*, 32–40.

Mukherjee, S., Pierson, T.C., and Dowd, K.A. (2014). Pseudo-infectious reporter virus particles for measuring antibody-mediated neutralization and enhancement of dengue virus infection. Methods Mol. Biol. *1138*, 75–97.

Nguyen, S.M., Antony, K.M., Dudley, D.M., Kohn, S., Simmons, H.A., Wolfe, B., Salamat, M.S., Teixeira, L.B.C., Wiepz, G.J., Thoong, T.H., et al. (2017). Highly efficient maternal-fetal Zika virus transmission in pregnant rhesus macaques. PLoS Pathog. *13*, e1006378.

Oliphant, T., Nybakken, G.E., Engle, M., Xu, Q., Nelson, C.A., Sukupolvi-Petty, S., Marri, A., Lachmi, B.E., Olshevsky, U., Fremont, D.H., et al. (2006). Antibody recognition and neutralization determinants on domains I and II of West Nile Virus envelope protein. J. Virol. *80*, 12149–12159.

Pal, P., Dowd, K.A., Brien, J.D., Edeling, M.A., Gorlatov, S., Johnson, S., Lee, I., Akahata, W., Nabel, G.J., Richter, M.K.S., et al. (2013). Development of a highly protective combination monoclonal antibody therapy against Chikungunya virus. PLoS Pathog. *9*, e1003312.

Pierson, T.C., and Diamond, M.S. (2013). Flaviviruses. In Fields Virology, D.M. Knipe and P.M. Howley, eds. (Lippincott Williams & Wilkins), pp. 747–794.

Pierson, T.C., Xu, Q., Nelson, S., Oliphant, T., Nybakken, G.E., Fremont, D.H., and Diamond, M.S. (2007). The stoichiometry of antibody-mediated neutralization and enhancement of West Nile virus infection. Cell Host Microbe *1*, 135–145.

Platt, D.J., Smith, A.M., Arora, N., Diamond, M.S., Coyne, C.B., and Miner, J.J. (2018). Zika virus-related neurotropic flaviviruses infect human placental explants and cause fetal demise in mice. Sci. Transl. Med. *10*, eaao7090.

Richner, J.M., Jagger, B.W., Shan, C., Fontes, C.R., Dowd, K.A., Cao, B., Himansu, S., Caine, E.A., Nunes, B.T.D., Medeiros, D.B.A., et al. (2017). Vaccine mediated protection against Zika virus-induced congenital disease. Cell *170*, 273–283.e12.

Rossi, S.L., Tesh, R.B., Azar, S.R., Muruato, A.E., Hanley, K.A., Auguste, A.J., Langsjoen, R.M., Paessler, S., Vasilakis, N., and Weaver, S.C. (2016). Characterization of a novel murine model to study Zika virus. Am. J. Trop. Med. Hyg. *94*, 1362–1369.

Rouvinski, A., Guardado-Calvo, P., Barba-Spaeth, G., Duquerroy, S., Vaney, M.C., Kikuti, C.M., Navarro Sanchez, M.E., Dejnirattisai, W., Wongwiwat, W., Haouz, A., et al. (2015). Recognition determinants of broadly neutralizing human antibodies against dengue viruses. Nature *520*, 109–113.

Sapparapu, G., Fernandez, E., Kose, N., Bin Cao, Fox, J.M., Bombardi, R.G., Zhao, H., Nelson, C.A., Bryan, A.L., Barnes, T., et al. (2016). Neutralizing human antibodies prevent Zika virus replication and fetal disease in mice. Nature *540*, 443–447.

Sheehan, K.C., Lai, K.S., Dunn, G.P., Bruce, A.T., Diamond, M.S., Heutel, J.D., Dungo-Arthur, C., Carrero, J.A., White, J.M., Hertzog, P.J., and Schreiber, R.D. (2006). Blocking monoclonal antibodies specific for mouse IFN-alpha/beta receptor subunit 1 (IFNAR-1) from mice immunized by in vivo hydrodynamic transfection. J. Interferon Cytokine Res. *26*, 804–819.

Suy, A., Sulleiro, E., Rodó, C., Vázquez, É., Bocanegra, C., Molina, I., Esperalba, J., Sánchez-Seco, M.P., Boix, H., Pumarola, T., and Carreras, E. (2016). Prolonged Zika virus viremia during pregnancy. N. Engl. J. Med. *375*, 2611–2613.

Taraphdar, D., Sarkar, A., Mukhopadhyay, B.B., and Chatterjee, S. (2012). A comparative study of clinical features between monotypic and dual infection cases with Chikungunya virus and dengue virus in West Bengal, India. Am. J. Trop. Med. Hyg. *86*, 720–723.

White, S.K., Lednicky, J.A., Okech, B.A., Morris, J.G., Jr., and Dunford, J.C. (2018). Spondweni virus in field-caught Culex quinquefasciatus mosquitoes, Haiti, 2016. Emerg. Infect. Dis. *24*, 1765–1767.

Zhao, H., Fernandez, E., Dowd, K.A., Speer, S.D., Platt, D.J., Gorman, M.J., Govero, J., Nelson, C.A., Pierson, T.C., Diamond, M.S., and Fremont, D.H. (2016). Structural basis of Zika virus-specific antibody protection. Cell *166*, 1016–1027.

STAR★METHODS

KEY RESOURCES TABLE

REAGENT or RESOURCE	SOURCE	IDENTIFIER
Antibodies		
Anti-mouse Ifnar1 monclonal	Leinco Technologies	Cat # MAR1-5A3
Alexa Fluor 488 anti-CD3e	Invitrogen	Cat # 53-0031-82
PerCP/Cy5.5 anti-CD8b	BioLegend	Cat # 126610
eFluor 450 anti-CD4	Invitrogen	Cat # 48-0041-82
APC/Cy7 anti-CD19	BioLegend	Cat # 115530
PE/Cy7 anti-CD44	BioLegend	Cat # 103030
Alexa Fluor 647 anti-IFNg	BioLegend	Cat # 505814
PE anti-granzyme B	Invitrogen	Cat # 12-8898-82
Anti-mouse CD16/32	BioLegend	Cat # 101310
Fixable Viability Dye eFluor 506	Invitrogen	Cat # 65-0866-14
BUV395 anti-CD45	BD Biosciences	Cat # 564279
Brilliant Violet 785 anti-CD4	BioLegend	Cat # 100551
Brilliant Violet 711 anti-B220	BioLegend	Cat # 101256
PE/Dazzle anti-CD11b	BioLegend	Cat # 101256
PE/Cy7 anti-CD11c	BD Biosciences	Cat # 558079
PerCP/Cy5.5 anti-Ly6G	BioLegend	Cat # 127616
Pacific Blue anti-Ly6C	BioLegend	Cat # 128014
PE anti-NK1.1	BioLegend	Cat # 108708
Alexa Fluor 700 anti-MHCII (I-A/E)	BioLegend	Cat # 107622
HRP-conjugated goat anti-mouse IgG	Sigma-Aldrich	Cat # A0168-1ML
Bacterial and Virus Strains		
Zika virus Dakar clone 41525-mouse adapted	Gorman et al., 2018	N/A
Spondweni virus SA Ar94	Haddow et al., 2016	GenBank: KX227370
Spondweni virus Chuku	Haddow et al., 2016	GenBank: KX227369
Chemicals, Peptides, and Recombinant Proteins		
RNA ISH SPOV probe	Advanced Cell Diagnostics	Cat # 512151
Brefeldin A solution (1000X)	BioLegend	Cat # 420601
TrueBlue Substrate	KPL	Cat # 5510-0030
Recombinant ZIKV envelope ectodomain	Native Antigen	Cat # ZIKVSU-ENV-100
Recombinant SPOV envelope ectodomain	This paper	N/A
ZIKV-derived, Db-restricted peptide $E_{294-302}$	Elong Ngono et al., 2017	N/A
Critical Commercial Assays		
TaqMan RNA-to-C_T 1 step kit	Applied Biosystems	Cat # 4392938
MagMAX-96 viral RNA isolation kit	Thermo Scientific	Cat # AM1836
Fixation/Permeabilization solution kit	BD Biosciences	Cat # 554714
Experimental Models: Cell Lines		
African green monkey kidney (Vero) cells	WHO reference cell bank	WHO Vero cells
HEK293T cells	ATCC	Cat # CRL-3216
Experimental Models: Organisms/Strains		
Mouse: C57BL/6J	Jackson Laboratory	Cat # 000664
Mouse: hSTAT2 KI	Gorman et al., 2018	N/A

(*Continued on next page*)

Continued

REAGENT or RESOURCE	SOURCE	IDENTIFIER
Oligonucleotides		
ZIKV-Dakar titering primers	Gorman et al., 2018	See Table S2
SPOV-SA Ar94 titering primers	This paper	See Table S2
SPOV-Chuku titering primers	This paper	See Table S2
Software and Algorithms		
Prism	GraphPad	Version 7.0h
FlowJo	FlowJo	Version 10.0.7

CONTACT FOR REAGENT AND RESOURCE SHARING

Further information and requests for resources and reagents should be directed to and will be fulfilled by the Lead Contact, Michael S. Diamond (diamond@wusm.wustl.edu).

EXPERIMENTAL MODEL AND SUBJECT DETAILS

Viruses

ZIKV strain Dakar 41525 (Senegal, 1984) and SPOV strains SA Ar94 (South Africa, 1955) and Chuku (Nigeria, 1952) were provided by the World Reference Center for Emerging Viruses and Arboviruses (R. Tesh and S. Weaver, University of Texas Medical Branch). The mouse-adapted ZIKV strain Dakar 41525 has been published (Gorman et al., 2018). Studies with SPOV and ZIKV were conducted under biosafety level 2 (BSL2) and animal (A-BSL3) containment at Washington University School of Medicine with Institutional Biosafety Committee approval.

SPOV and ZIKV stocks were propagated in Vero cells after inoculating at a multiplicity of infection (MOI) of 0.01 and incubating at 37°C for 40 h. Virus stocks were propagated in mycoplasma-free Vero cells and titrated by focus-forming assay. Infected cell foci were detected at 48 h after infection, following fixation with 1% paraformaldehyde and incubation with 500 ng/ml of flavivirus cross-reactive mouse monoclonal antibody E60 (Oliphant et al., 2006) for 2 h at room temperature. After incubation for 1 h with a 1:5,000 dilution of horseradish peroxidase (HRP)-conjugated goat anti-mouse IgG (Sigma), foci were detected by addition of True Blue substrate (KPL). Foci were analyzed with a CTL ImmunoSpot instrument.

Recombinant viral proteins

ZIKV envelope (E) ectodomain (strain French Polynesia, 2013) was purchased commercially (Native Antigen). A fragment of the open reading frame from Spondweni virus strain SM-6 V-1 (NCBI Reference Sequence YP_009222008.1) encoding E protein residues 2-412 was inserted into pET21(a) between the NdeI and XhoI sites. The clone contains a methionine codon for initiation contributed by the NdeI site and a stop codon before the XhoI site. The protein was produced in BL21(DE3) cells after a 4 h induction with 1 mM IPTG at 37°C and refolded in arginine buffer following a published protocol (Zhao et al., 2016).

Serum from ZIKV- and DENV-immune subjects

We studied nine subjects in the United States with previous ZIKV (n = 5) or DENV (n = 4) infection. No sample size estimation was performed for these studies. Subjects were allocated to experimental groups based on their known infection status. The studies were approved by the Institutional Review Board of Vanderbilt University Medical Center; samples were obtained after informed consent was obtained by the Vanderbilt Clinical Trials Center.

Ethics statement for mouse studies

This study was carried out in accordance with the recommendations in the Guide for the Care and Use of Laboratory Animals of the National Institutes of Health. The protocols were approved by the Institutional Animal Care and Use Committee at the Washington University School of Medicine (Assurance number A3381-01). Inoculations were performed under anesthesia induced and maintained with ketamine hydrochloride and xylazine, and all efforts were made to minimize animal suffering.

Mouse infection experiments

WT C57BL/6 mice were purchased commercially (Jackson Laboratory, 000664). Eight week-old mice were inoculated by subcutaneous route in the footpad with 10^6 (SPOV-SA Ar94) or 10^5 (SPOV-Chuku) focus-forming units (FFU) in a volume of 50 μl. One-day prior to virus inoculation, mice were treated with 0.5, 1, 1.5, or 2 mg of an Ifnar1-blocking mAb (MAR1-5A3 (Sheehan et al., 2006)) by intraperitoneal injection. Survival and weight loss were monitored for 21 days, and some animals were harvested at 7 dpi for viral burden analysis. In some experiments, mice were administered before (day −1) or after (day +1) virus inoculation a single 100 μg (4 mg/kg)

dose of cross-reactive human IgG1 mAbs (ZIKV-117 (Sapparapu et al., 2016), EDE1-A9 (Barba-Spaeth et al., 2016), EDE1-B10 (Fernandez et al., 2017), EDE1-C4 (Barba-Spaeth et al., 2016), ZIKV-A7 or ZIKV-C10 (W.D. and G.R.S., unpublished data), or an isotype control humanized mAb (hu-CHK-152 (Pal et al., 2013)) or LALA (leucine to alanine substitutions) variants (Fernandez et al., 2017; Sapparapu et al., 2016).

For pregnancy studies, WT C57BL/6 male and female mice were mated. At embryonic day E5.5, dams were treated with 0.5 or 1 mg anti-Ifnar1 mAb by intraperitoneal injection. At E6.5, dams were inoculated with 10^6 FFU of SPOV-SA Ar94 by a subcutaneous route in the footpad. Animals were euthanized at E13.5 or E18, and placentas, fetuses, and maternal tissues were harvested depending on the experiment.

METHOD DETAILS

Measurement of viral burden

SPOV-infected mice were euthanized at 7, 14, or 21 dpi and perfused extensively with 20 mL of PBS. Brain, spleen, testis, kidney, ileum, and eye tissues were harvested, weighed, and homogenized with zirconia beads in a MagNA Lyser instrument (Roche Life Science) in 300 μL of DMEM media supplemented with 2% heat-inactivated FBS. Blood was collected and allowed to clot at room temperature; serum was separated, and all tissue homogenates were clarified by centrifugation at 6,000 x *g* for 5 min and stored at −80°C. RNA was extracted using an Applied Biosystems 5x MagMax RNA 96 viral isolation kit (Thermo Scientific) and a Kingfisher duo prime extraction machine (Thermo Scientific). With some samples, viral burden was determined by plaque assay on Vero cells as described (Miner et al., 2016) except 2% methylcellulose instead of agarose was used for the overlay. ZIKV RNA levels were determined by one-step quantitative reverse transcriptase PCR (qRT–PCR) using an Applied Biosystems Taqman RNA-to-Ct 1-step kit (Thermo Scientific) on an ABI 7500 Fast Instrument using standard cycling conditions. Previously designed primer/probe sets were used for the SPOV (Haddow et al., 2016) and ZIKV Dakar 41525 (Lanciotti et al., 2008) strains, and primer/probe sets were designed for the SPOV strains (Table S1). Viral burden was expressed on a $\log_{10}$ scale as ZIKV RNA equivalents per gram or ml after comparison with a standard curve produced using serial tenfold dilutions of ZIKV RNA (Govero et al., 2016). Separate standard curves were made for each SPOV strain.

Histology and RNA *in situ* hybridization

Placentas and fetuses from uninfected or SPOV-infected pregnant mice (E13.5) were collected, fixed overnight in 4% paraformaldehyde (PFA) in PBS, and cut into 3-μm-thick sections followed by hematoxylin and eosin (H&E) staining. RNA ISH was performed using RNAscope 2.5 (Advanced Cell Diagnostics) according to the manufacturer's instructions. PFA-fixed paraffin-embedded tissue sections were deparaffinized by incubating for 60 min at 60 °C. Endogenous peroxidases were quenched with H_2O_2 for 10 min at room temperature. Slides were boiled for 15 min in RNAscope Target Retrieval Reagents and incubated for 30 min in RNAscope Protease Plus before probe hybridization. The probe targeting SPOV RNA was designed and synthesized by Advanced Cell Diagnostics (Catalog #512151). Tissues were counterstained with Gill's hematoxylin and visualized using bright-field microscopy.

RVP neutralization and enhancement assays

Pseudo-infectious RVP production has been described previously (Mukherjee et al., 2014). Briefly, RVPs were produced by the co-tranfection of a GFP-expressing WNV sub-genomic replicon with an expression vector encoding viral structural proteins (C-prM-E) *in trans* using HEK293T cells. Virus-containing supernantants were harvested and filtered 3 to 7 days post-transfection. Plasmids encoding the structural genes (ZIKV, H/PF/2013; SPOV, SM-6 V-1; DENV2, 16681) were generated using previously described methods (Ansarah-Sobrinho et al., 2008; Dowd et al., 2016). RVPs were diluted sufficiently to ensure antibody excess and incubated with an equivalent volume of serially diluted mouse or human serum or mAbs for 1 h at 37°C. The resulting immune complexed were used to infect Raji-DCSIGNR cells and incubated at 37°C for 36 to 48 h. Cells were fixed with ~3% paraformaldehyde, and GFP expression was detected by flow cytometry. The resulting data was analyzed and dose-response curves were fit using nonlinear regression to calculate the sera dilution required to inhibit infection by 50% (EC_{50}) (Prism 7 Software; GraphPad). To measure antibody-dependent enhancement antibody-RVP immune complexes were generated as described above and used to infect Fc-γ receptor-expressing K562 cells for 36 to 48 h at 37°C. RVPs were fixed, infection was detected by flow cytometry and scored as a function of GFP expression.

Antibody-virus neutralization assays

Serial dilutions of mAbs were incubated with 10^2 FFU of different SPOV strains for 1 h at 37°C. The mAb–virus complexes were added to Vero cell monolayers in 96-well plates for 1 h at 37°C. Subsequently, cells were overlaid with 1% (w/v) methylcellulose in MEM. Plates were fixed 40 h later with 1% PFA in PBS for 1 h at room temperature. The plates were incubated with 500 ng/ml of E60 and developed in a focus-forming assay as described above. For serum antibody neutralization assays, both SPOV and ZIKV-immune mouse sera were heat-inactivated for 30 min at 60°C. Sera then was diluted in 96-well round bottom (1:20, 1:60, 1:180, 1:540, 1:620, 1:4860, 1:14580) and mixed with SPOV SA Ar94 or ZIKV Dakar 41525 (10^2 FFU of SPOV or ZIKV per well). Samples were added to Vero cell monolayers in 96-well plates and processed by focus-forming assay as described above.

Antibody responses

The levels of SPOV and ZIKV-specific IgM and IgG were determined using an ELISA against purified SPOV and ZIKV E protein, respectively. Polystyrene ELISA plates were coated with 4 μg/ml of recombinant SPOV or ZIKV E protein. Plates were blocked with 2% BSA in PBS containing 0.05% Tween-20 (blocking buffer), and then incubated for at least 1 h. Heat-inactivated serum samples from SPOV or ZIKV-infected mice were diluted in blocking buffer and then incubated for at least 2 h. Bound antibodies were detected using biotin-labeled goat anti-mouse IgM and IgG antibodies and streptavidin-HRP. End-point titers for SPOV and ZIKV E-specific IgM and IgG concentration were defined as reciprocal serum dilutions that corresponded to two times the average OD values obtained with BSA.

T cell assays

Splenocytes from naive, SPOV, and ZIKV-infected mice at 8 days after infection were plated (1×10^6 per well, in 200 μl) in 96-well round-bottom plates and stimulated with 1 μg of an immunodominant ZIKV-derived, D^b-restricted peptide $E_{294\text{-}302}$ for 6 h at 37°C in the presence of brefeldin A, as previously detailed (Elong Ngono et al., 2017). Cells without stimulation and splenocytes from naive animals were used as negative controls. After incubation, cells were stained with antibodies against CD3ε (Alexa Fluor 488, 145-2C11, BioLegend, 1:100), CD4 (eFluor 450, GK1.5, Invitrogen, 1:100), CD8β (PerCP/Cy5.5, YTS156.7.7, BioLegend, 1:200), CD19 (APC/Cy7, 6D5, BioLegend, 1:200), and CD44 antigens (PE/Cy7, IM7, BioLegend, 1:100). After fixation and permeabilization using Cytofix/Cytoperm buffer (BD Biosciences), cells were incubated with anti-IFNγ (Alexa Fluor 647, XMG1.2, BioLegend, 1:100), and anti-granzyme B (PE, GB11, Invitrogen, 1:100) mAbs. Samples were processed on a LSRII flow cytometer and analyzed using FlowJo software X 10.0.7.

Flow cytometric analysis

Uninfected and SPOV-Chuku infected mice (both treated with 1 mg anti-Ifnar1 at day −1) were euthanized at 5 dpi and perfused extensively with 20 mL of PBS. The inoculated foot was skinned and disarticulated from the tibia. Tissues were incubated for 2 h at 37°C in RPMI with collagenase (2.5 mg/mL, Sigma, C-0130), DNase I (Sigma, D5025), and 10% FBS. Digested tissue was passed through a 100-μm strainer, and cells were separated by centrifugation (200 x g, 5 min). Cells were incubated with antibodies to CD16/32 (93, Biolegend, 1:100) for 10 min at 4°C and then stained with a fixable viability dye (eFluor 506, eBioscience) and antibodies to CD45 (BUV395, 30-F11, BD Biosciences, 1:200), CD3ε (Alexa Fluor 488, 145-2C11, BioLegend, 1:200), CD4 (Brilliant Violet 785, RM4-5, Biolegend, 1:200), CD8β (PerCP/Cy5.5, YTS156.7.7, BioLegend, 1:200), B220 (Brilliant Violet 711, RA3-6B2, Biolegend, 1:200), CD11b (PE/Dazzle, M1/70, Biolegend, 1:200), CD11c (PE-Cy7, HL3, BD Biosciences, 1:200), Ly6G (PerCP/Cy5.5, 1A8, Biolegend, 1:400), Ly6C (Pacific Blue, HK1.4, 1:200, Biolegend), NK1.1 (PE, PK136, Biolegend, 1:200), and MHCII (Alexa Fluor 700, M5/114.15.2, Biolegend, 1:200). Datasets were acquired on a LSRII flow cytometer and analyzed using FlowJo software X 10.0.7.

QUANTIFICATION AND STATISTICAL ANALYSIS

Data analysis

All statistical analysis was performed with GraphPad Prism software. Details of statistical tests used to analyze experiments are described in the Figure Legends. Kaplan-Meier survival curves were analyzed by the log rank test with a Bonferroni post-test, and weight change or foot swelling was evaluated with a Kruskal-Wallis ANOVA with a Dunnett's post-test correction. For viral burden analysis, the $\log_{10}$ transformed titers were analyzed by Mann–Whitney test or a Kruskal–Wallis ANOVA with Dunn's post-test correction. A *P value* of < 0.05 established statistically significant differences.

DATA AND SOFTWARE AVAILABILITY

All data is available upon request to the lead contact author. No proprietary software was used in the data analysis.